SUPPORTING INFORMATION

Ruthenium half-sandwich type complexes with bidentate monosaccharide ligands show antineoplastic activity in ovarian cancer cell models through reactive oxygen species production

István Kacsir[#1,2], Adrienn Sipos[#3], Gyula Ujlaki[3], Péter Buglyó[4], László Somsák[1], Péter Bai*[3,5,6], Éva Bokor*[1]

[1]Department of Organic Chemistry, University of Debrecen, PO Box 400, H-4002 Debrecen, Hungary;
[2]Doctoral School of Chemistry, University of Debrecen, PO Box 400, H-4002 Debrecen, Hungary;
[3]Department of Medical Chemistry, Faculty of Medicine, University of Debrecen, H-4032 Debrecen, Hungary;
[4]Department of Inorganic & Analytical Chemistry, Faculty of Sciences and Technology, University of Debrecen, H-4032 Debrecen, Hungary;
[5]NKFIH-DE Lendület Laboratory of Cellular Metabolism, H-4032 Debrecen, Hungary;
[6]Research Center for Molecular Medicine, Faculty of Medicine, University of Debrecen, H-4032 Debrecen, Hungary
[#]equal contribution

*corresponding authors

Correspondence should be sent to:
Éva Bokor, PhD, University of Debrecen, Department of Organic Chemistry, , PO Box 400, H-4002 Debrecen, Hungary, Tel. +36 52 512 900 ext 22474; e-mail: bokor.eva@science.unideb.hu

Péter Bai, PhD, DSc University of Debrecen, Department of Medical Chemistry, H-4032 Debrecen, Egyetem tér 1., Hungary, Tel. +36 52 412 345; Fax. +36 52 412 566, e-mail: baip@med.unideb.hu

Table of contents:

1. Selected NMR data for the synthesized compounds

Table S1. Selected ^{1}H NMR data of **Ru-dimer**, the 1-(β-D-glucopyranosyl)-4-hetaryl-1,2,3-triazoles (**L-1**–**L-3**) and their half-sandwich Ru(II) complexes (**Ru-1**–**Ru-3**)

	Tria-H-5	Py-H-6	Py-H-4 or Qu-H-4	H-1'	H-2'	*p*-cym-CH_{Ar}	*i*-Pr-CH	C_6H_4-C*H*$_3$	*i*-Pr-CH_3
Ru-dimer ($CDCl_3$)	-	-	-	-	-	5.48; 5.34	2.93	2.16	1.28
Ru-dimer (CD_3OD)	-	-	-	-	-	5.88; 5.66	3.31	2.20	1.30
Ru-dimer (DMSO-d_6)	-	-	-	-	-	5.81; 5.77	2.82	2.08	1.18
L-1a ($CDCl_3$)	8.42	8.61	7.78	5.94	5.51	-	-	-	-
L-1b ($CDCl_3$)	8.63	-	8.24	5.99	5.59	-	-	-	-
L-2a ($CDCl_3$)	8.61	8.61	7.86-7.76*	6.34	6.07	-	-	-	-
L-3a (CD_3OD)	8.63	8.59	7.92	5.70	3.96	-	-	-	-
L-3b (DMSO-d_6)	8.99	-	8.51	5.68	3.90	-	-	-	-
Ru-1a ($CDCl_3$)	8.92; 8.79	9.25; 9.22	7.96	6.00; 5.99	5.95-5.88*	5.95-5.83, 5.73-5.67*	2.79; 2.74	2.22; 2.20	1.17-1.12*
Ru-1b ($CDCl_3$)	9.03; 9.24	-	8.39; 8.37	6.08; 6.11	6.03; 5.97	5.96-5.67*	2.57; 2.53	2.07; 2.15	1.07, 1.04; 1.02, 1.00
Ru-2a ($CDCl_3$)	9.02; 8.98	9.23; 9.20	7.82-7.75*	6.50; 6.43	6.60; 6.10	5.81-5.44*	2.50; 2.36	2.08; 2.00	0.94, 0.91; 0.79, 0.74
Ru-3a (CD_3OD)	9.22; 9.21	9.42	8.19	5.88; 5.88	3.95-3.89*	6.12-6.05, 5.90-5.84*	2.79-2.71*	2.22	1.18-1.09*
Ru-3b (DMSO-d_6)	9.42; 9.41	-	8.70; 8.68	5.95; 5.93	4.00; 3.99	6.13-5.96*	2.48; 2.46	2.20	1.00, 0.98; 0.92, 0.92

*Overlapping signals.

Table S2. Changes of the chemical shifts of selected ^{1}H NMR resonances as a result of the complex formation for **Ru-1**–**Ru-3** ($\Delta = \delta_{complex} - \delta_{ligand\ or\ \textbf{Ru-dimer}}$).

Triazolok	Δ(Tria-H-5)	Δ(Py-H-6)	Δ(Py-H-4) or Δ(Qu-H-4)	Δ(H-1')	Δ(H-2')	*i*-Pr-CH	C_6H_4-C*H*$_3$	*i*-Pr-CH_3
Ru-1a ($CDCl_3$)	+0.50 +0.37	+0.64 +0.61	+0.18	+0.06 +0.05	*	-0.14 -0.19	+0.06 +0.04	*
Ru-1b ($CDCl_3$)	+0.40 +0.61	-	+0.15 +0.13	+0.09 +0.12	+0.44 +0.38	-0.36 -0.40	-0.09 -0.01	-0.21, -0.24 -0.26, -0.28
Ru-2a ($CDCl_3$)	+0.41 +0.37	+0.62 +0.59	*	+0.16 +0.09	+0.53 +0.03	-0.43 -0.57	-0.08 -0.16	-0.34, -0.37 -0.49, -0.54
Ru-3a (CD_3OD)	+0.59 +0.58	+0.83	+0.27	+0.18 +0.18	*	*	+0.02	*
Ru-3b (DMSO-d_6)	+0.43 +0.42	-	+0.19 +0.17	+0.27 +0.25	+0.10 +0.09	-0.34; -0.36	+0.12	-0.18, -0.20 -0.26, -0.26

*Due to signal overlaps these resonances could not be assigned precisely.

Table S3. Selected ^{13}C NMR data of **Ru-dimer**, the 1-(β-D-glucopyranosyl)-4-hetaryl-1,2,3-triazoles (**L-1**–**L-3**) and their half-sandwich Ru(II) complexes (**Ru-1**–**Ru-3**)

	Tria-C-5	Py-C-6	Py-C-5	Py-C-4 or Qu-C-4	Py-C-3 or Qu-C-3	C-1'	C-2'	*p*-cym-C_{qAr}	*p*-cym-CH_{Ar}	*i*-Pr-*C*H	C_6H_4-*C*H_3
Ru-dimer ($CDCl_3$)	-	-	-	-	-	-	-	101.2; 96.8	81.3; 80.5	30.6	19.0
Ru-dimer (CD_3OD)	-	-	-	-	-	-	-	102.7; 98.5	80.4; 79.3	32.6	18.9
Ru-dimer (DMSO-d_6)	-	-	-	-	-	-	-	106.4; 100.1	86.4; 85.5	30.0	17.9
L-1a ($CDCl_3$)	120.7	149.7	123.3	137.0	120.5	86.0	70.7	-	-	-	-
L-1b ($CDCl_3$)	121.4	-	-	137.0	118.7	86.0	70.7	-	-	-	-
L-2a ($CDCl_3$)	121.0	149.6	123.3	137.1	120.6	86.4	71.3	-	-	-	-
L-3a (CD_3OD)	123.4	150.5	124.6	138.9	121.7	89.8	74.1	-	-	-	-
L-3b (DMSO-d_6)	123.3	-	-	137.3	118.3	87.8	72.2	-	-	-	-
Ru-1a ($CDCl_3$)	125.4; 125.3	155.5; 155.4	127.1; 126.9	140.3; 140.2	122.9	86.8; 86.7	70.2; 69.8	106.3, 101.8; 105.5, 103.1	86.4-83.1*	31.1; 31.0	18.7
Ru-1b ($CDCl_3$)	127.6; 127.5	-	-	141.0; 141.3	119.1; 118.8	88.1-84.0*	70.2; 69.8	105.4, 102.7; 106.3, 102.1	88.1-84.0*	31.1; 31.3	18.5; 18.7
Ru-2a ($CDCl_3$)	126.2; 123.8	155.7; 155.5	127.2; 126.9	140.1; 140.0	122.7	87.2; 86.7	71.7; 70.4	105.8, 102.6; 105.3, 103.9	86.4-82.5*	31.0	18.8; 18.6
Ru-3a (CD_3OD)	125.5; 125.2	156.8	127.6	141.5	123.6	91.3; 91.2	74.5; 74.3	106.8, 103.8; 106.6, 104.1	87.3-84.6*	32.3; 32.2	18.8; 18.7
Ru-3b (DMSO-d_6)	127.1; 126.9	-	-	142.6	119.5; 119.4	91.4; 91.2	74.4; 74.3	106.5, 104.7; 106.3, 104.9	88.6-84.3*	32.3; 32.2	18.8; 18.7

*Signals were not assigned precisely.

Table S4. Changes of the chemical shifts of selected ^{13}C NMR resonances as a result of the complex formation for **Ru-1**–**Ru-3** ($\Delta = \delta_{complex} - \delta_{ligand\ or\ \textbf{Ru-dimer}}$)

	Δ(Tria-C-5)	Δ(Py-C-6)	Δ(Py-C-5)	Δ(Py-C-4) or Δ(Qu-C-4)	Δ(Py-C-3) or Δ(Qu-C-3)	Δ(C-1')	Δ(C-2')	Δ (*p*-cym-C_{qAr})	Δ(*i*-Pr-CH)	Δ(C_6H_4-C*H*$_3$)
Ru-1a ($CDCl_3$)	+4.7 +4.6	+5.8 +5.7	+3.8 +3.6	+3.3 +3.2	+2.4	+0.8 +0.7	-0.5 -0.9	+5.1, +5.0 +4.3, +4.6	+0.5 +0.4	-0.3
Ru-1b ($CDCl_3$)	+6.2 +6.1	-	-	+4.0 +4.3	+0.4 +0.1	*	-0.5 -0.9	+4.2, +5.9 +5.1, +5.3	+0.5 +0.7	-0.5 -0.3
Ru-2a ($CDCl_3$)	+5.2 +2.8	+6.1 +5.9	+3.9 +3.6	+3.0 +2.9	+2.1	+0.8 +0.3	+0.4 +0.1	+4.6, +5.8 +4.1, +7.1	+0.4	-0.2 -0.4
Ru-3a (CD_3OD)	+2.1 +1.8	+6.3	+3.0	+2.6	+1.9	+1.5 +1.4	+0.4 +0.2	+4.1, +5.3 +3.9, +5.6	-0.3 -0.4	-0.1 -0.2
Ru-3b (DMSO-d_6)	+3.8 +3.6	-	-	+5.3	+1.2 +1.1	+3.6 +3.4	+0.2 +0.1	+0.1; +4.6 -0.1; +4.8	+2.3; +2.2	+0.9 +0.8

*Due to uncertain signal assignment the data could not be calculated precisely.

Table S5. Selected ^{1}H NMR data of **Ru-dimer**, the monosaccharide-based 5-(pyridine-2-yl)-1,3,4-oxadiazoles (**L-4**–**L-12**) and their half-sandwich Ru(II) complexes (**Ru-4**–**Ru-12**)

	Py-H-6	Py-H-5	H-1'	H-2'	*p*-cym-CH_{Ar}	*i*-Pr-CH	C_6H_4-C*H*$_3$
Ru-dimer ($CDCl_3$)	-	-	-	-	5.48; 5.34	2.93	2.16
Ru-dimer (CD_3OD)	-	-	-	-	5.88; 5.66	3.31	2.20
L-4 ($CDCl_3$)	8.81	7.48	5.28	6.05	-	-	-
L-5 ($CDCl_3$)	8.82	7.49	4.92	5.56	-	-	-
L-6 ($CDCl_3$)	8.80	7.47	5.15	5.96	-	-	-
L-7 ($CDCl_3$)	8.82	7.50	4.89	5.67	-	-	-
L-8 ($CDCl_3$)	8.81	7.47	5.30	6.32	-	-	-
L-9 ($CDCl_3$)	8.79	7.49	6.35	5.69	-	-	-
L-10 (CD_3OD)	8.75	7.64	4.68	3.84	-	-	-
L-11 (CD_3OD)	8.74	7.63	4.59	3.84	-	-	-
L-12 (CD_3OD)	8.77	7.65	4.63	4.22	-	-	-
Ru-4 ($CDCl_3$)	9.26; 9.50	7.77; 7.91	5.46; 5.35	6.16; 5.72	5.90-5.51*	2.78; 2.72	1.95; 2.02
Ru-5 ($CDCl_3$)	9.30; 9.45	7.80; 7.88	5.03; 5.00	5.75; 5.44	6.01-5.96, 5.82-5.69*	3.03; 2.91	2.23-2.02*
Ru-6 ($CDCl_3$)	9.26; 9.46	7.77; 7.89	5.28; 5.24	6.11; 5.74	5.86-5.35*	2.80; 2.75	1.99; 2.04
Ru-7 ($CDCl_3$)	9.34; 9.46	7.80; 7.87	5.01; 4.98	5.85; 5.47	6.01-5.95, 5.82-5.71*	3.01; 2.89	2.24-2.04*
Ru-8 ($CDCl_3$)	9.26; 9.49	7.80; 7.93	5.47; 5.37	6.43; 6.02-5.94*	5.84-5.27*	2.80; 2.73	1.94; 2.03
Ru-9 ($CDCl_3$)	9.33	7.79	6.52; 6.46	5.84-5.71*	6.01-5.95, 5.84-5.71*	2.98; 2.97	2.29-2.08*
Ru-10 (CD_3OD)	9.54	7.95; 7.94	4.85; 4.83	3.83; 3.81	6.19-6.13, 5.94-5.92*	2.91; 2.90	2.23
Ru-11 (CD_3OD)	9.53	7.95-7.92*	4.77; 4.76	3.81; 3.80	6.18-6.12, 5.94-5.90*	2.91	2.22
Ru-12 (CD_3OD)	9.55	7.95; 7.94	4.78; 4.76	4.18; 4.15	6.19-6.13, 5.94-5.92*	2.91	2.23

*Overlapping signals.

Table S6. Changes of the chemical shifts of selected ^{1}H NMR resonances as a result of the complex formation for **Ru-4**–**Ru-12** ($\Delta = \delta_{complex} - \delta_{ligand\ or\ \textbf{Ru-dimer}}$)

	Δ(Py-H-6)	Δ(Py-H-5)	Δ(H-1')	Δ(H-2')	Δ(*i*-Pr-CH)	Δ(C_6H_4-C*H*$_3$)
Ru-4 ($CDCl_3$)	+0.45 +0.69	+0.29 +0.43	+0.18 +0.07	+0.11 -0.33	-0.15 -0.21	-0.21 -0.14
Ru-5 ($CDCl_3$)	+0.48 +0.63	+0.31 +0.39	+0.11 +0.08	+0.19 -0.12	+0.10 -0.02	*
Ru-6 ($CDCl_3$)	+0.46 +0.66	+0.30 +0.42	+0.13 +0.09	+0.15 -0.22	-0.13 -0.18	-0.17 -0.12
Ru-7 ($CDCl_3$)	+0.52 +0.64	+0.30 +0.37	+0.12 +0.09	+0.18 -0.20	+0.08 -0.04	*
Ru-8 ($CDCl_3$)	+0.45 +0.68	+0.33 +0.46	+0.17 +0.07	+0.11 *	-0.13 -0.20	-0.22 -0.13
Ru-9 ($CDCl_3$)	+0.54	+0.30	+0.17 +0.11	*	+0.05 +0.04	*
Ru-10 (CD_3OD)	+0.79	+0.31 +0.30	+0.17 +0.15	-0.01 -0.03	-0.40 -0.41	+0.03
Ru-11 (CD_3OD)	+0.79	*	+0.18 +0.17	-0.03 -0.04	-0.40	+0.02
Ru-12 (CD_3OD)	+0.78	+0.30 +0.29	+0.15 +0.13	-0.04 -0.07	-0.40	+0.03

*Due to signal overlaps these resonances could not be assigned precisely.

Table S7. Selected ^{13}C NMR data of **Ru-dimer**, the monosaccharide-based 5-(pyridine-2-yl)-1,3,4-oxadiazoles (**L-4**–**L-12**) and their half-sandwich Ru(II) complexes (**Ru-4**–**Ru-12**)

	Py-C-6	Py-C-5	Py-C-4	Py-C-3	Py-C-2	*p*-cym-C_{qAr}	*p*-cym-CH_{Ar}	*i*-Pr-*C*H	C_6H_4-*C*H_3
Ru-dimer ($CDCl_3$)	-	-	-	-	-	101.2; 96.8	81.3; 80.5	30.6	19.0
Ru-dimer (CD_3OD)	-	-	-	-	-	102.7; 98.5	80.4; 79.3	32.6	18.9
L-4 ($CDCl_3$)	150.5	126.2	137.3	123.5	143.2	-	-	-	-
L-5 ($CDCl_3$)	150.6	126.3	137.4	123.6	143.2	-	-	-	-
L-6 ($CDCl_3$)	150.6	126.2	137.3	123.5	143.3	-	-	-	-
L-7 ($CDCl_3$)	150.5	126.2	137.3	123.6	143.2	-	-	-	-
L-8 ($CDCl_3$)	150.5	126.2	137.3	123.6	143.3	-	-	-	-
L-9 ($CDCl_3$)	150.4	126.3	137.4	123.5	143.1	-	-	-	-
L-10 (CD_3OD)	151.4	127.9	139.3	124.5	144.0	-	-	-	-
L-11 (CD_3OD)	151.4	127.9	139.3	124.5	144.0	-	-	-	-
L-12 (CD_3OD)	151.4	127.9	139.3	124.5	144.1	-	-	-	-
Ru-4 ($CDCl_3$)	156.6; 158.3	131.2-128.5*	140.1; 140.3	125.2; 125.3	140.2; 139.1	104.8, 102.1; 107.0, 102.3	88.7-83.2; 85.5-83.6*	31.1; 31.3	18.1; 18.8
Ru-5 ($CDCl_3$)	156.4; 157.6	130.0; 130.8	140.3; 140.5	125.4; 125.5	140.3; 139.5	105.0, 102.4; 106.4, 102.7	88.2-83.1*	31.2; 31.3	18.3; 18.8
Ru-6 ($CDCl_3$)	157.0; 157.9	130.8-128.5*	140.3; 140.4	125.1, 125.2	140.0; 139.3	104.9, 102.1; 106.3, 102.4	88.4-83.1*	31.0; 31.2	18.1; 18.6
Ru-7 ($CDCl_3$)	156.5; 157.4	129.9; 130.5	140.1; 140.3	125.2; 125.3	139.9; 139.2	105.1, 102.2; 106.2, 102.6	87.6-82.9; 85.7-83.0*	31.0; 31.1	18.1; 18.5
Ru-8 ($CDCl_3$)	156.3; 157.9	130.9-128.5*	140.2; 140.3	125.2; 125.3	140.2; 139.3	104.7, 102.0; 106.8, 102.3	88.8-83.0*	31.1; 31.3	18.0; 18.7
Ru-9 ($CDCl_3$)	156.9; 156.8	130.3	140.4	125.4; 125.3	139.8; 139.7	105.9, 102.4; 105.7, 102.3	87.2-83.3*	31.3	18.5; 18.4
Ru-10 (CD_3OD)	158.3	131.1	142.0	126.6; 126.5	141.6; 141.5	107.3, 103.5 107.2, 103.4	87.4-84.8*	32.4	18.8
Ru-11 (CD_3OD)	158.2	131.1	142.0	126.6; 126.5	141.6; 141.5	107.4, 103.5 107.4, 103.4	87.4-84.8*	32.4	18.7
Ru-12 (CD_3OD)	158.1	131.1	141.9	126.5; 126.4	141.6; 141.5	107.4, 103.5 107.3, 103.4	87.2-84.7*	32.4	18.7

*Signals were not assigned precisely.

Table S8. Changes of the chemical shifts of selected ^{13}C NMR resonances as a result of the complex formation for **Ru-4**–**Ru-12** ($\Delta = \delta_{complex} - \delta_{ligand\ or\ \textbf{Ru-dimer}}$)

	Δ(Py-C-6)	Δ(Py-C-5)	Δ(Py-C-4)	Δ(Py-C-3)	Δ(Py-C-2)	Δ(*p*-cym-C_{qAr})	*i*-Pr-*C*H	C_6H_4-*C*H_3
Ru-4 ($CDCl_3$)	+6.1 +7.8	*	+2.8 +3.0	+1.7 +1.8	-3.0 -4.1	+3.6, +5.3 +5.8, +5.5	+0.5 +0.7	-0.9 -0.2
Ru-5 ($CDCl_3$)	+5.8 +7.0	+3.7 +4.5	+2.9 +3.1	+1.8 +1.9	-2.9 -3.7	+3.8, +5.6 +5.2, +5.9	+0.6 +0.7	-0.7 -0.2
Ru-6 ($CDCl_3$)	+6.4 +7.3	*	+3.0 +3.1	+1.6 +1.7	-3.3 -4.0	+3,7, +5.3 +5.1, +5.6	+0.4 +0.6	-0.9 -0.4
Ru-7 ($CDCl_3$)	+6.0 +6.9	+3.7 +4.3	+2.8 +3.0	+1.6 +1.7	-3.3 -4.0	+3.9, +5.4 +5.0, +5.8	+0.4 +0.5	-0.9 -0.5
Ru-8 ($CDCl_3$)	+5.8 +7.4	*	+2.9 +3.0	+1.6 +1.7	-3.1 -4.0	+3.5, +5.2 +5.6, +5.5	+0.5 +0.7	-1.0 -0.3
Ru-9 ($CDCl_3$)	+6.5 +6.4	+4.0	+3.0	+1.9 +1.8	-3.3 -3.4	+4.7, +5.6 +4.5, +5.5	+0.7	-0.5 -0.6
Ru-10 (CD_3OD)	+6.9	+3.2	+2.7	+2.1 +2.0	-2.4 -2.5	+4.6, +5.0 +4.5, +4.9	-0.2	-0.1
Ru-11 (CD_3OD)	+6.8	+3.2	+2.7	+2.1 +2.0	-2.4 -2.5	+4.7, +5.0 +4.7, +4.9	-0.2	-0.2
Ru-12 (CD_3OD)	+6.7	+3.2	+2.6	+2.0 +1.9	-2.5 -2.6	+4.7, +5.0 +4.6, +4.9	-0.2	-0.2

*Due to uncertain signal assignment the data could not be calculated precisely.

2. Copies of ^{1}H and ^{13}C NMR spectra

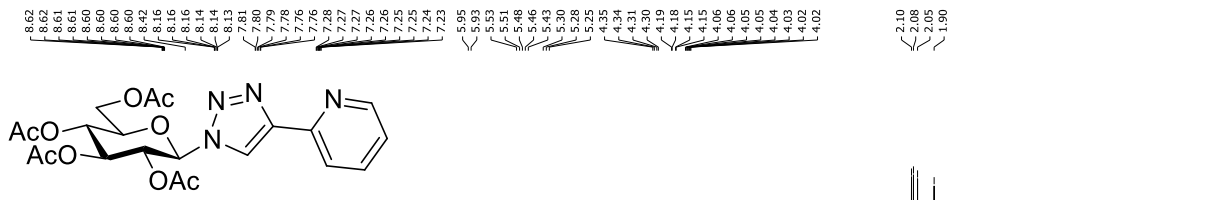

L-1a ($CDCl_3$, 360 MHz)

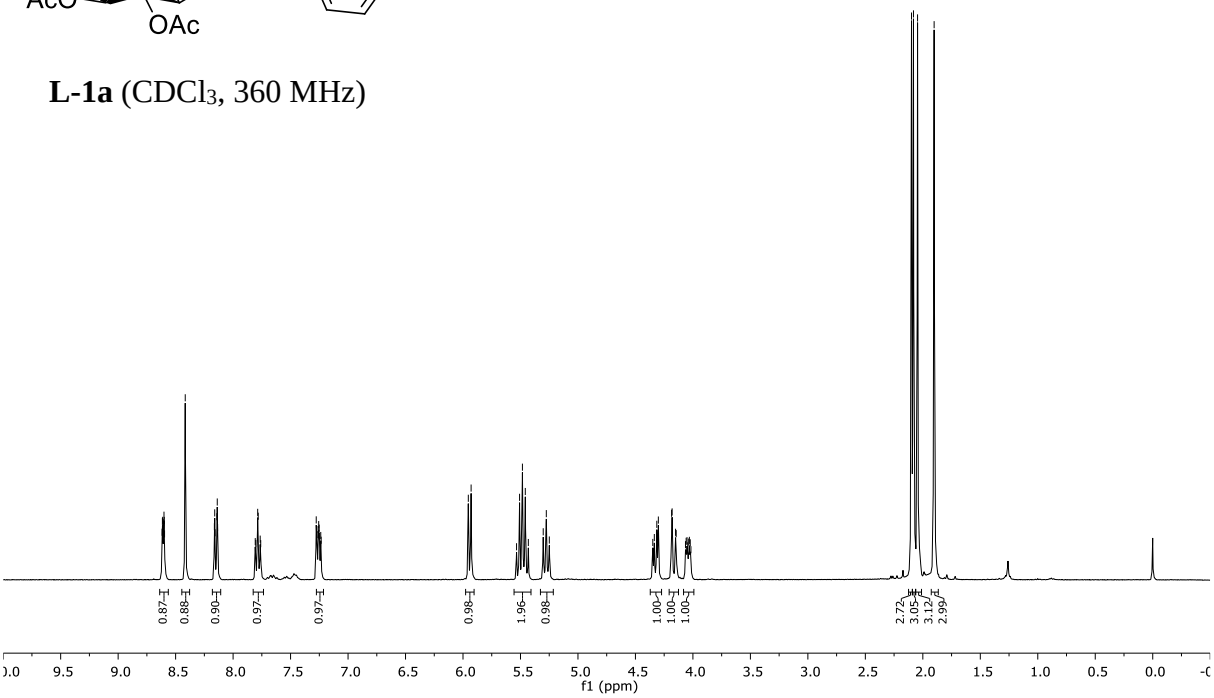

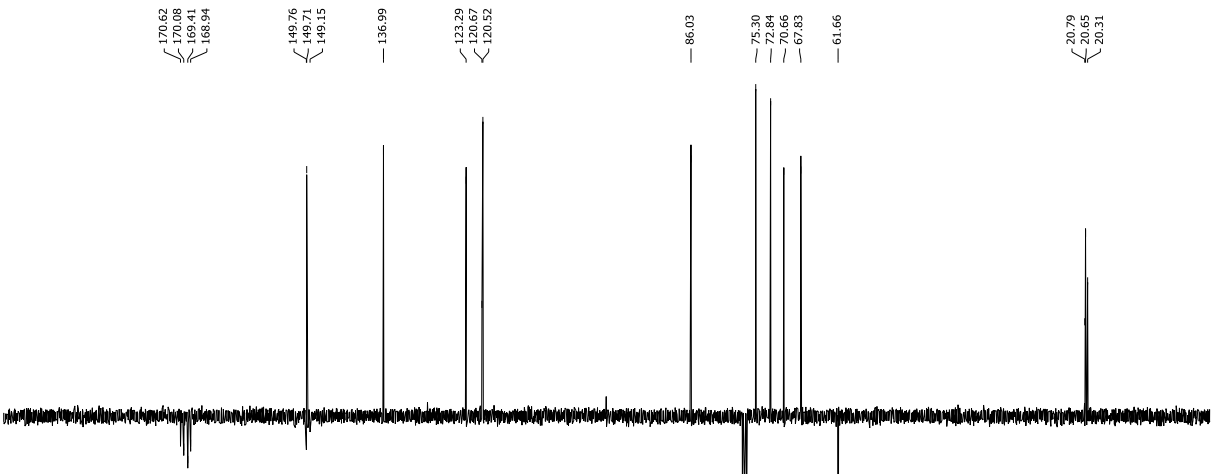

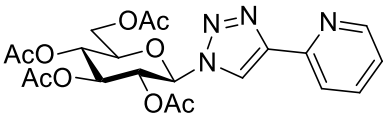

L-1a ($CDCl_3$, 90 MHz)

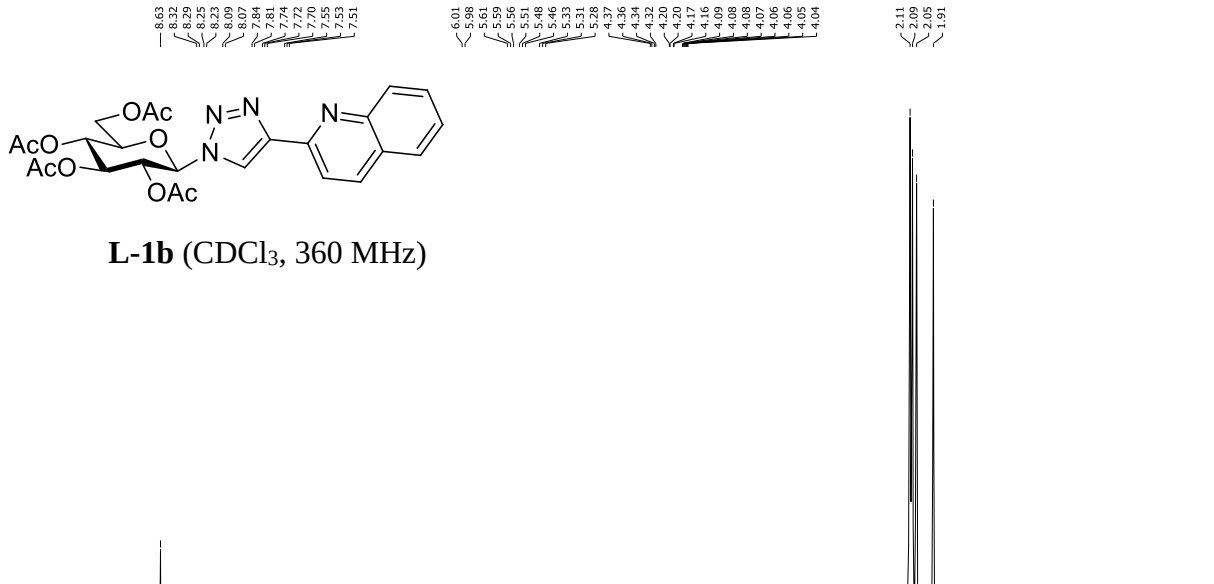

L-1b ($CDCl_3$, 360 MHz)

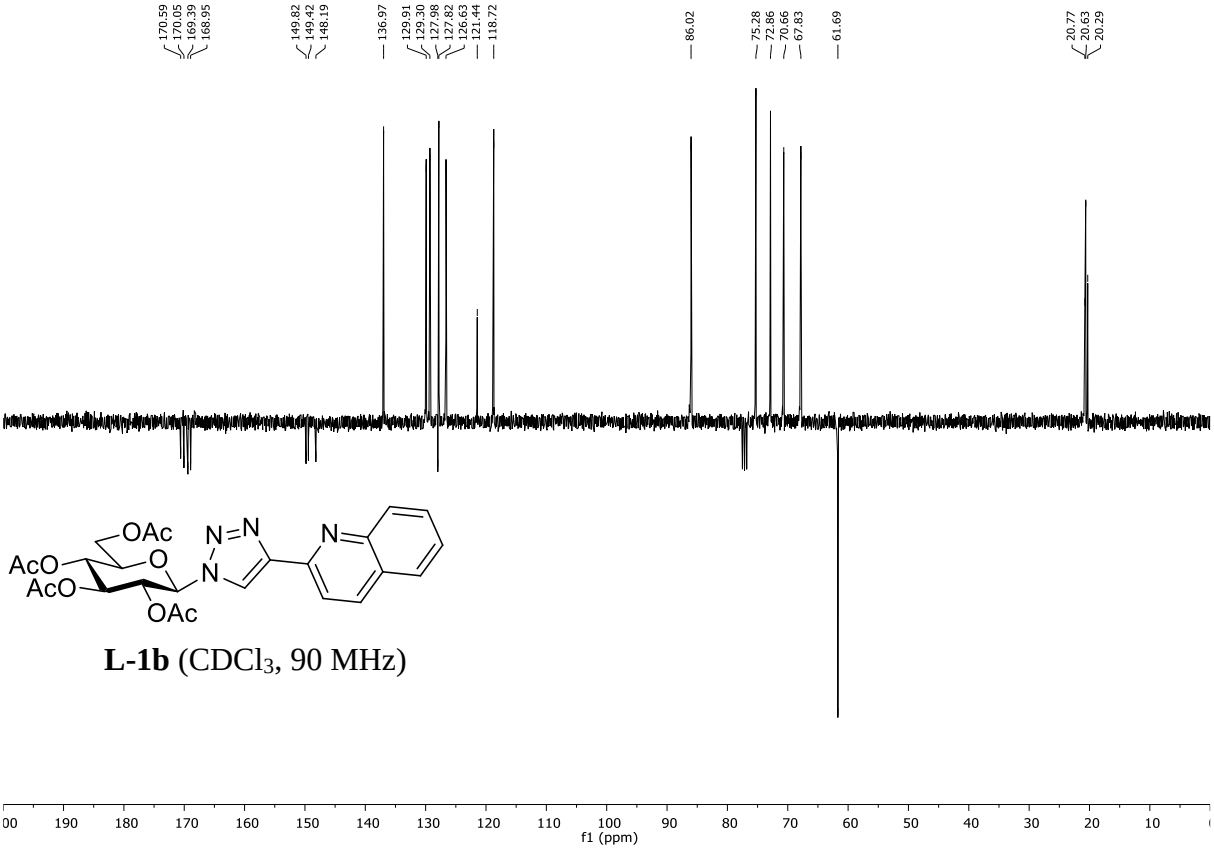

L-1b ($CDCl_3$, 90 MHz)

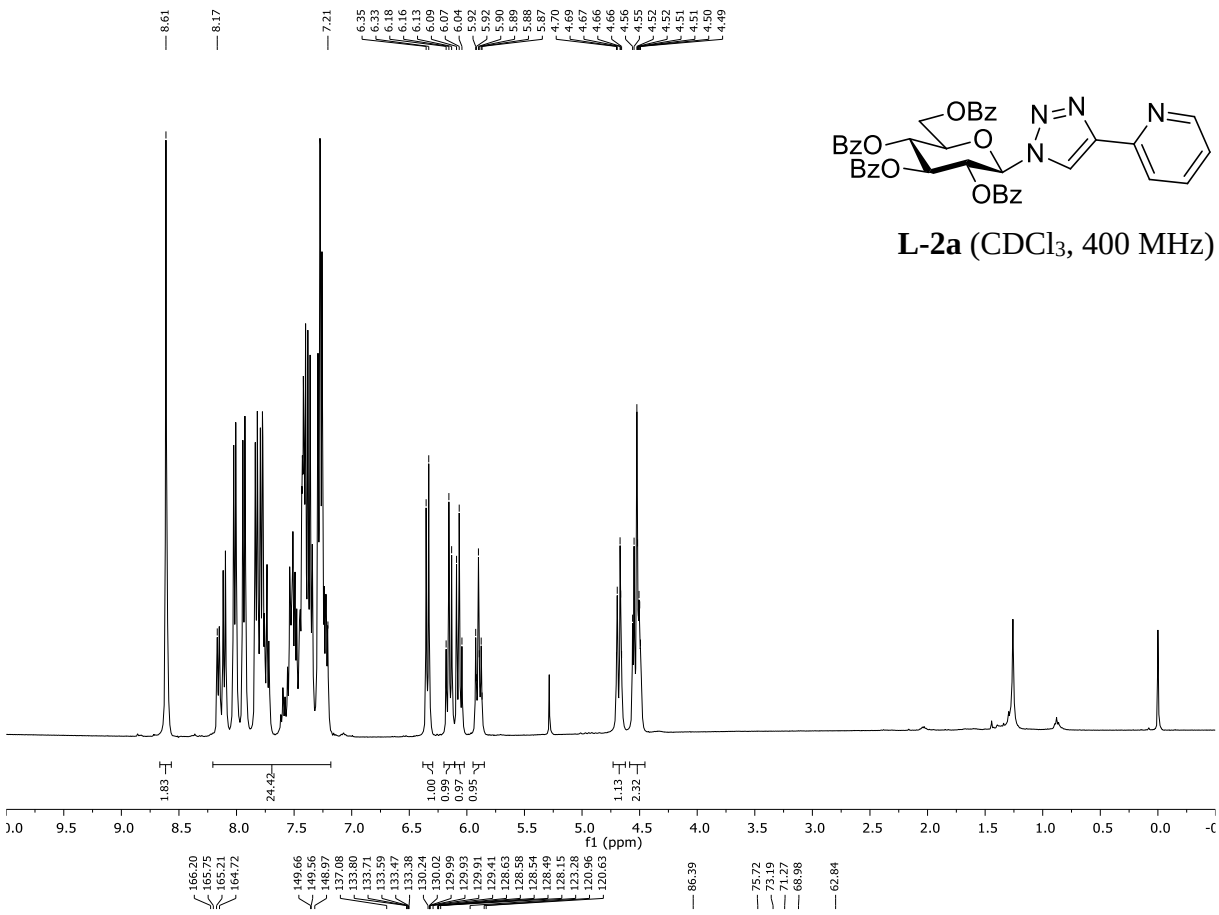

L-2a ($CDCl_3$, 400 MHz)

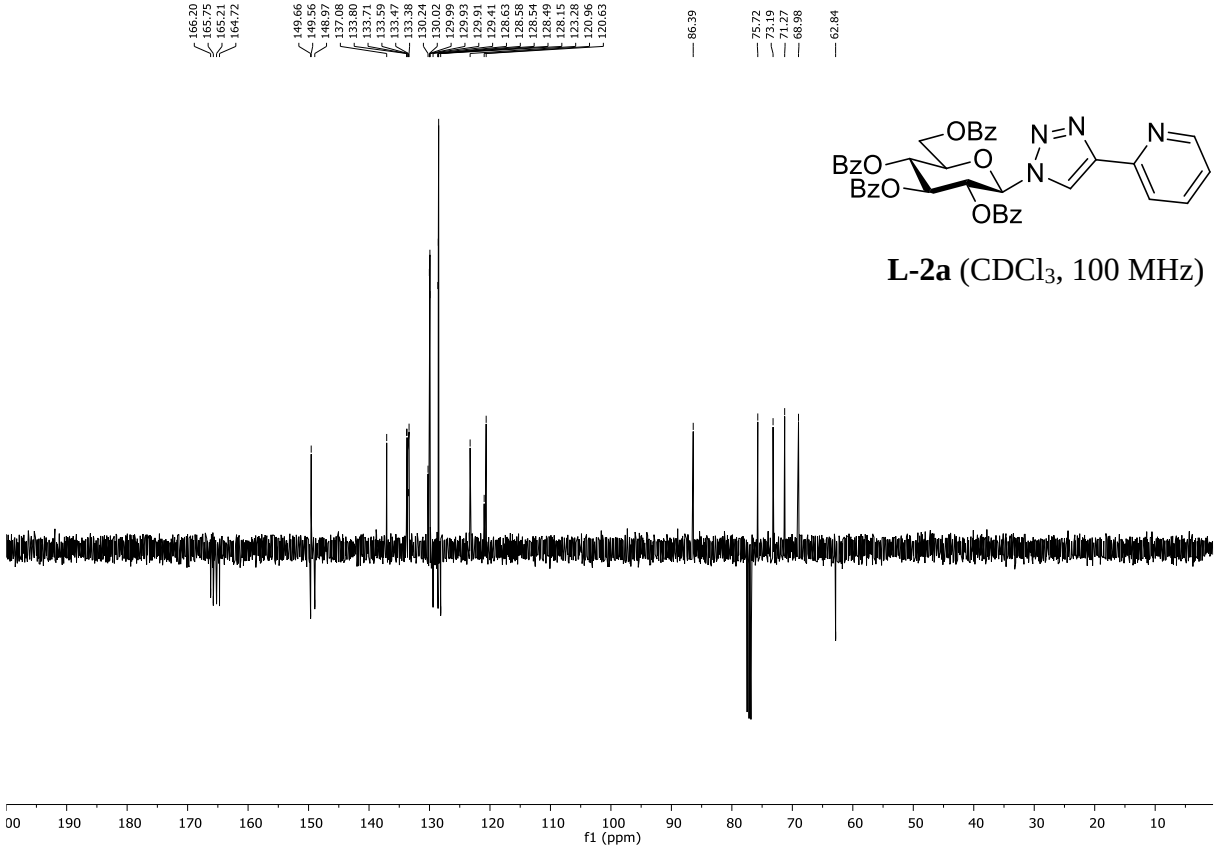

L-2a ($CDCl_3$, 100 MHz)

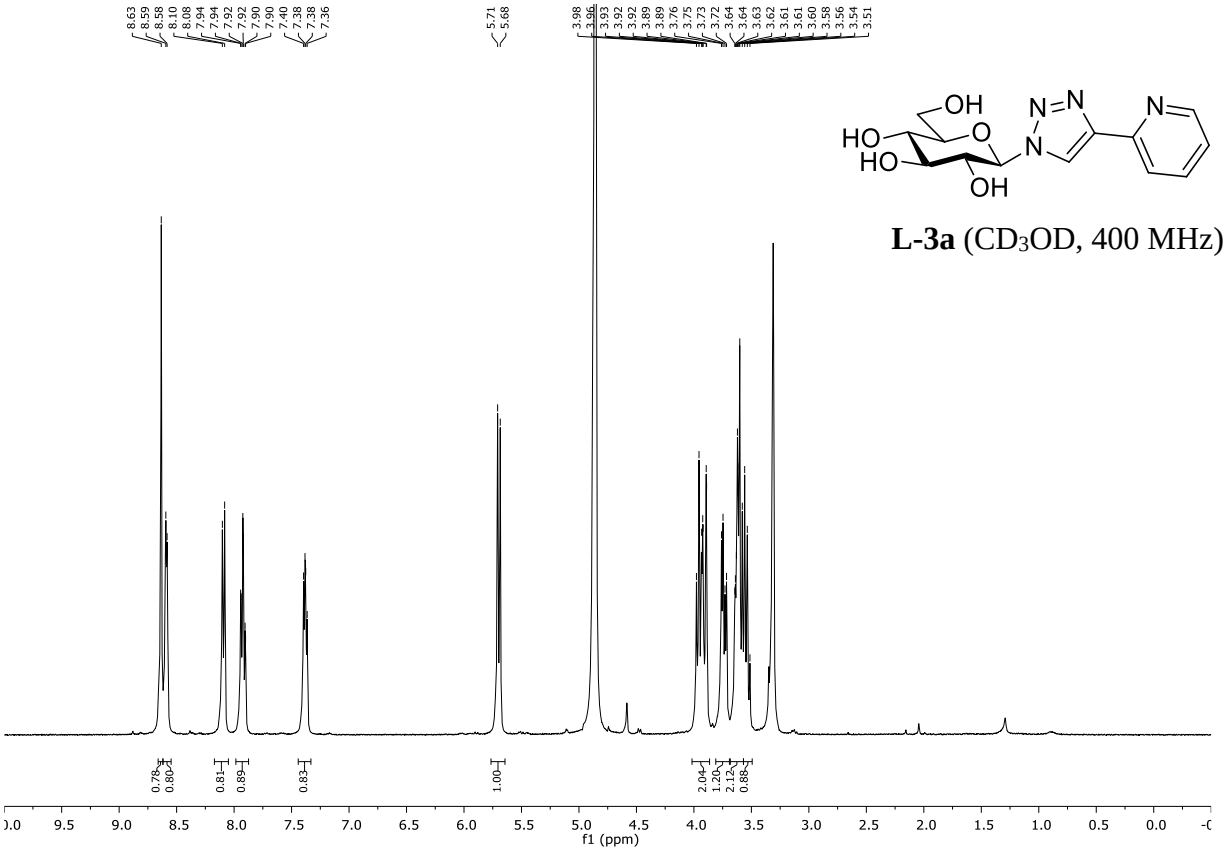

L-3a (CD_3OD, 400 MHz)

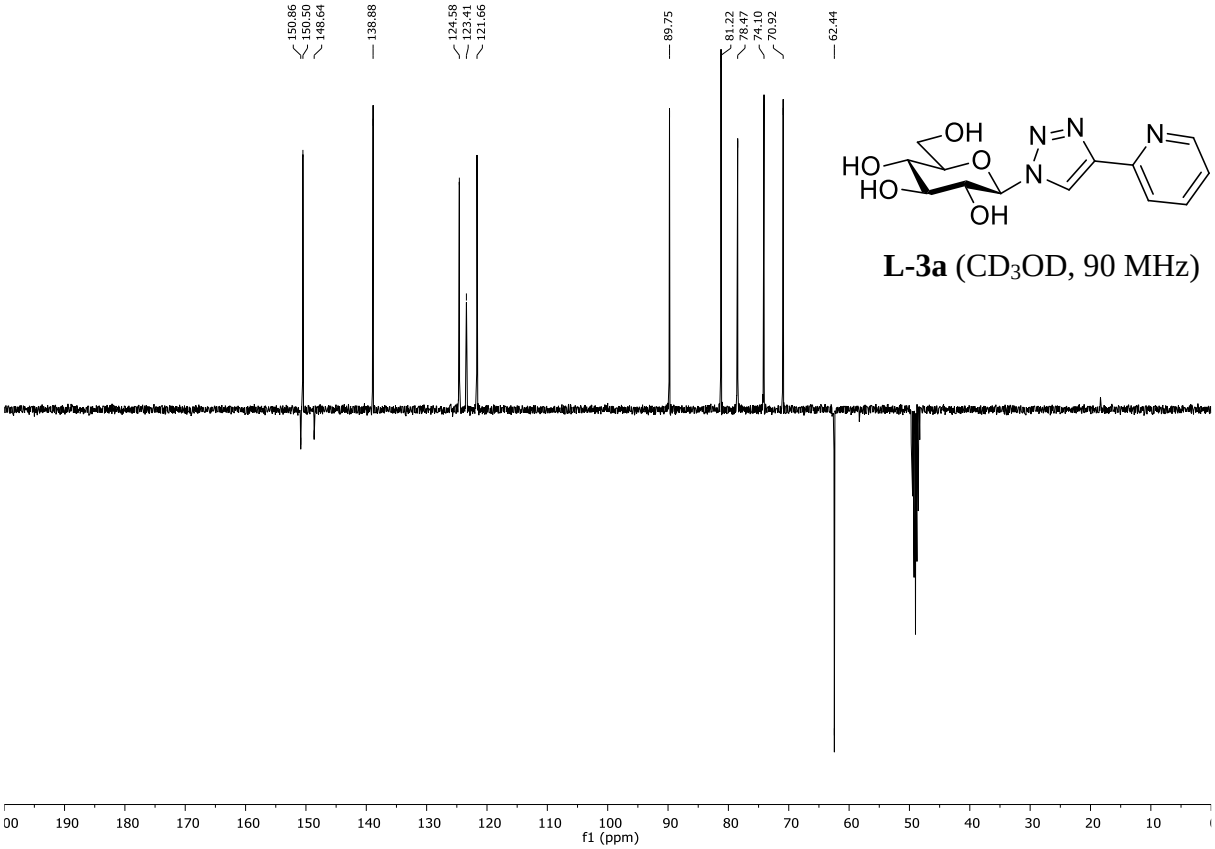

L-3a (CD_3OD, 90 MHz)

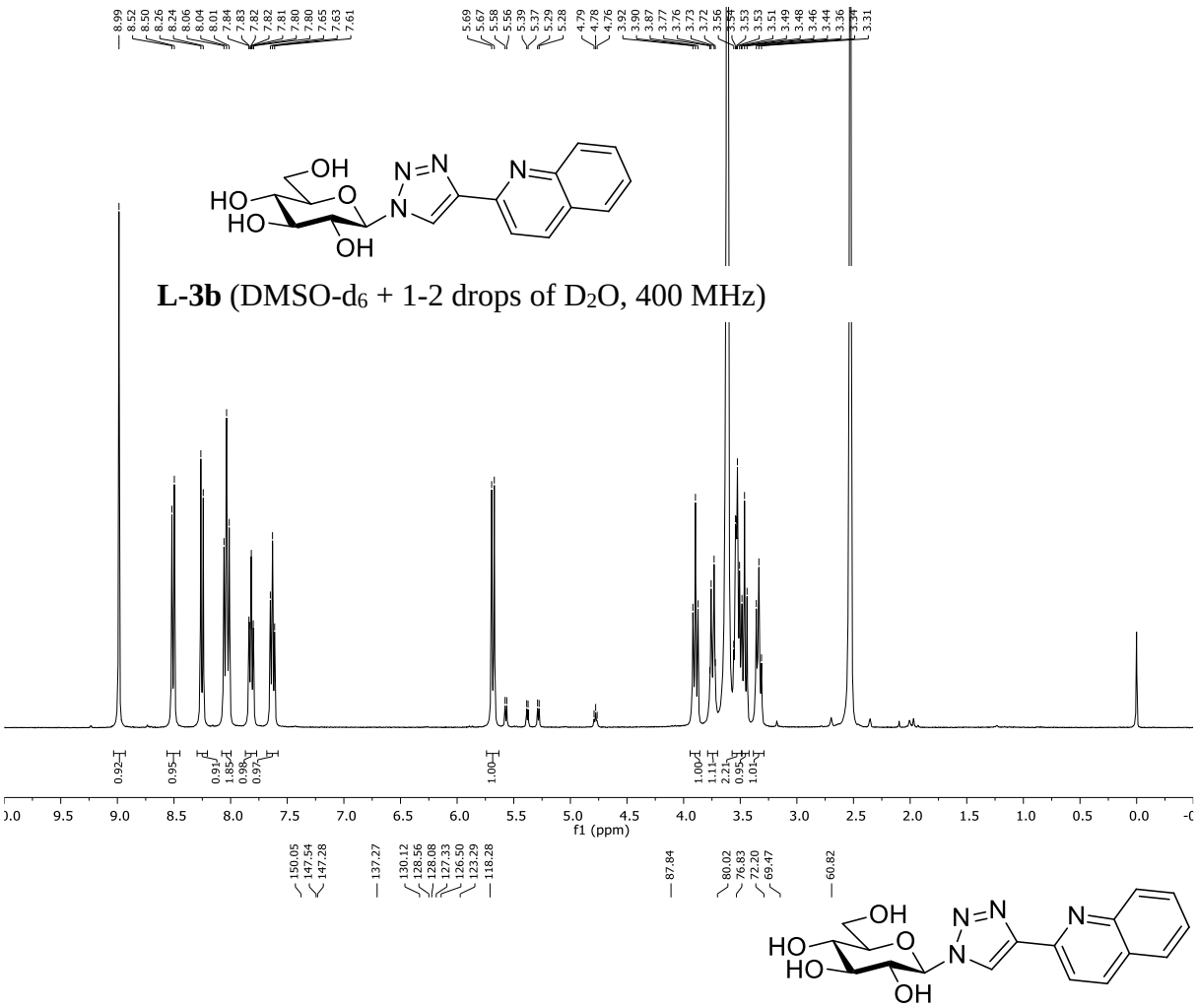

L-3b (DMSO-d_6 + 1-2 drops of D_2O, 400 MHz)

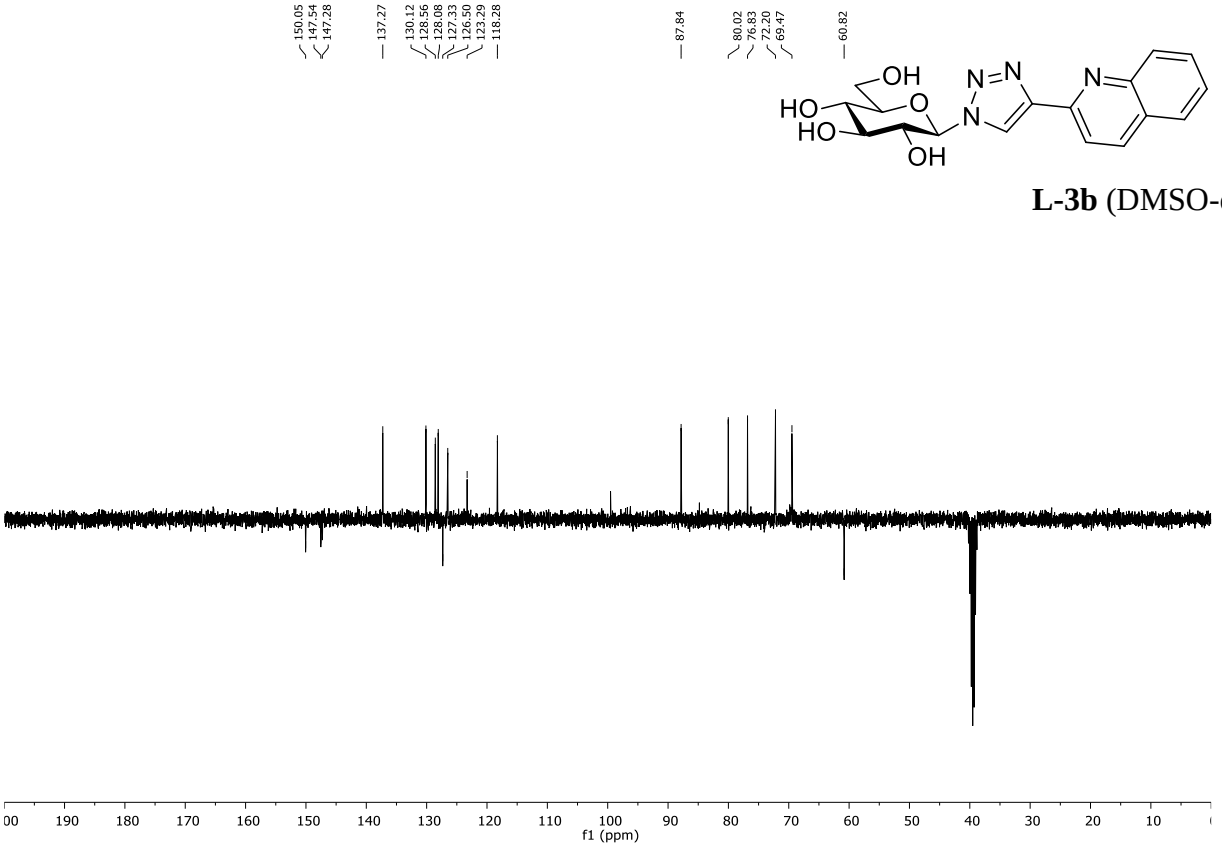

L-3b (DMSO-d_6, 90 MHz)

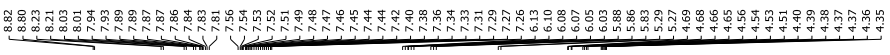

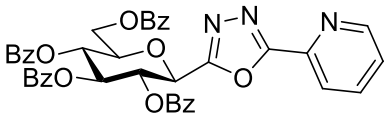

L-4 ($CDCl_3$, 400 MHz)

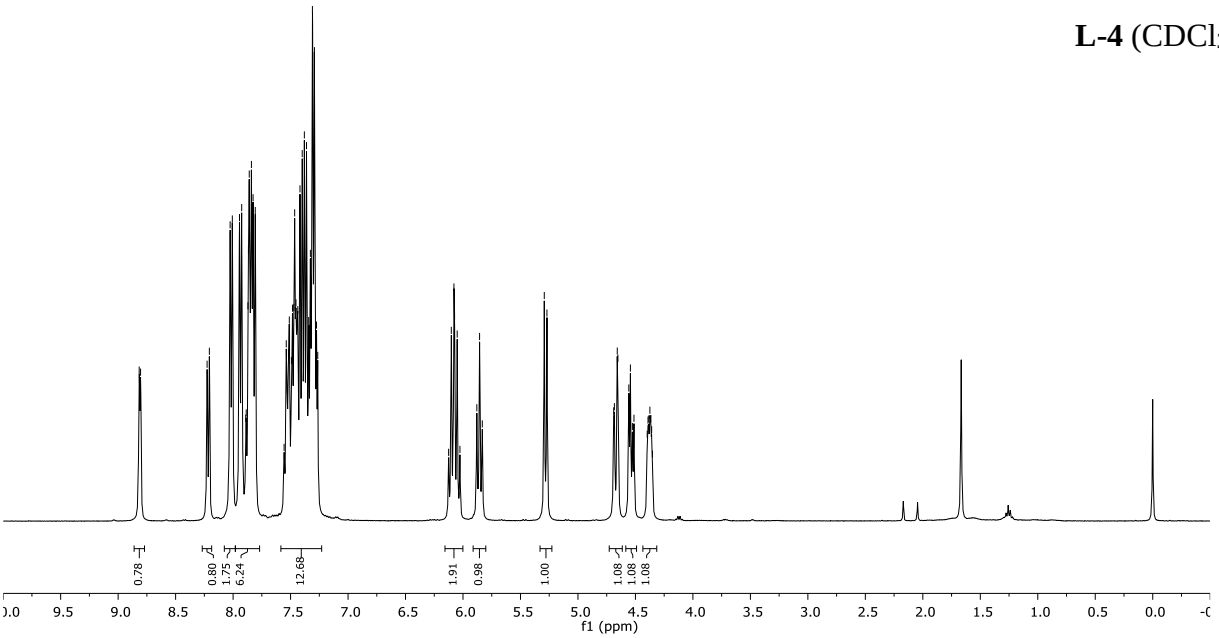

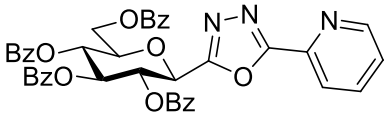

L-4 ($CDCl_3$, 90 MHz)

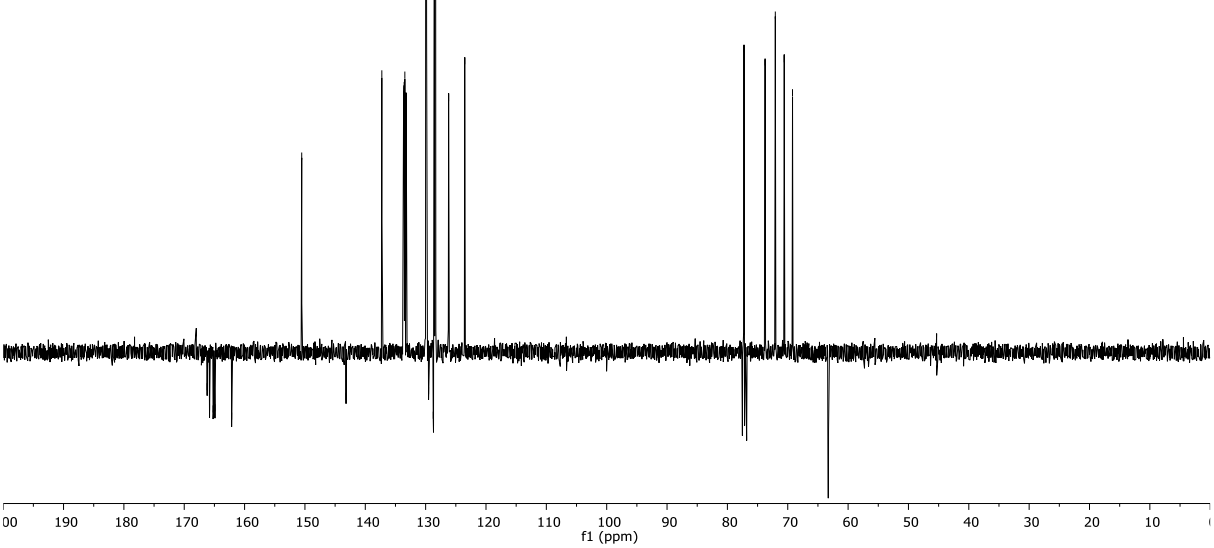

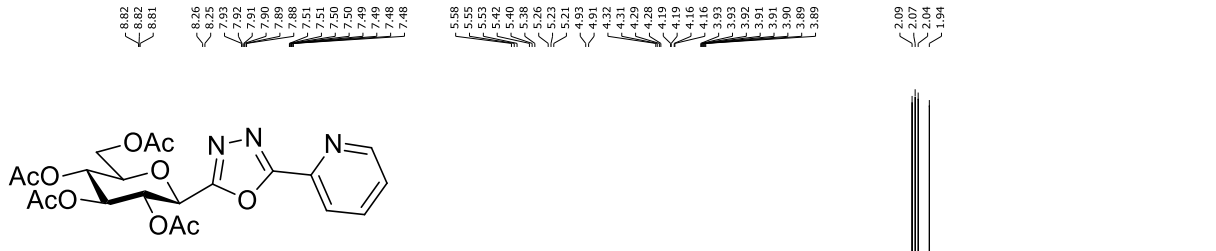

L-5 ($CDCl_3$, 400 MHz)

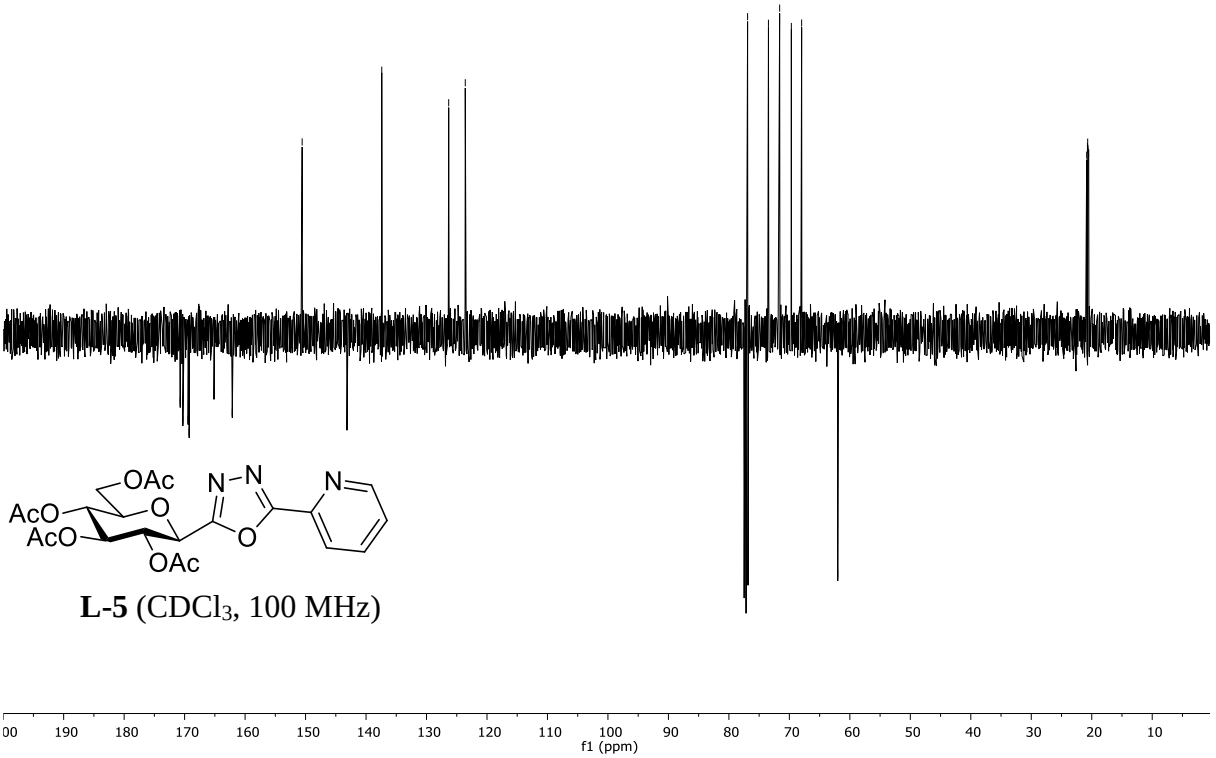

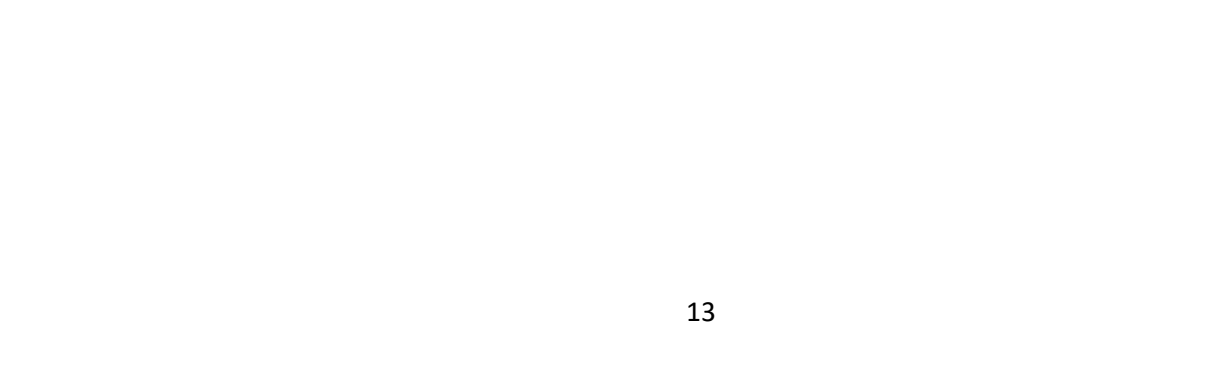

L-5 ($CDCl_3$, 100 MHz)

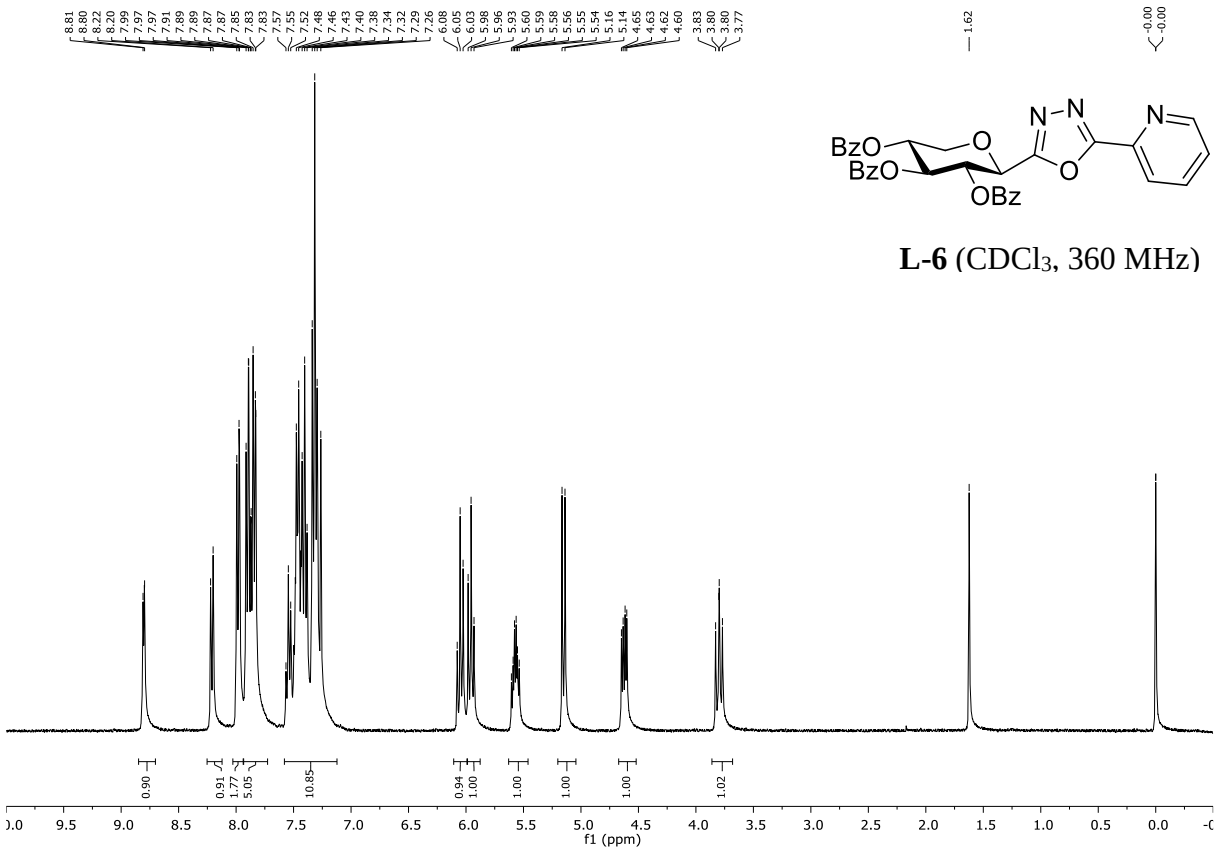

L-6 ($CDCl_3$, 360 MHz)

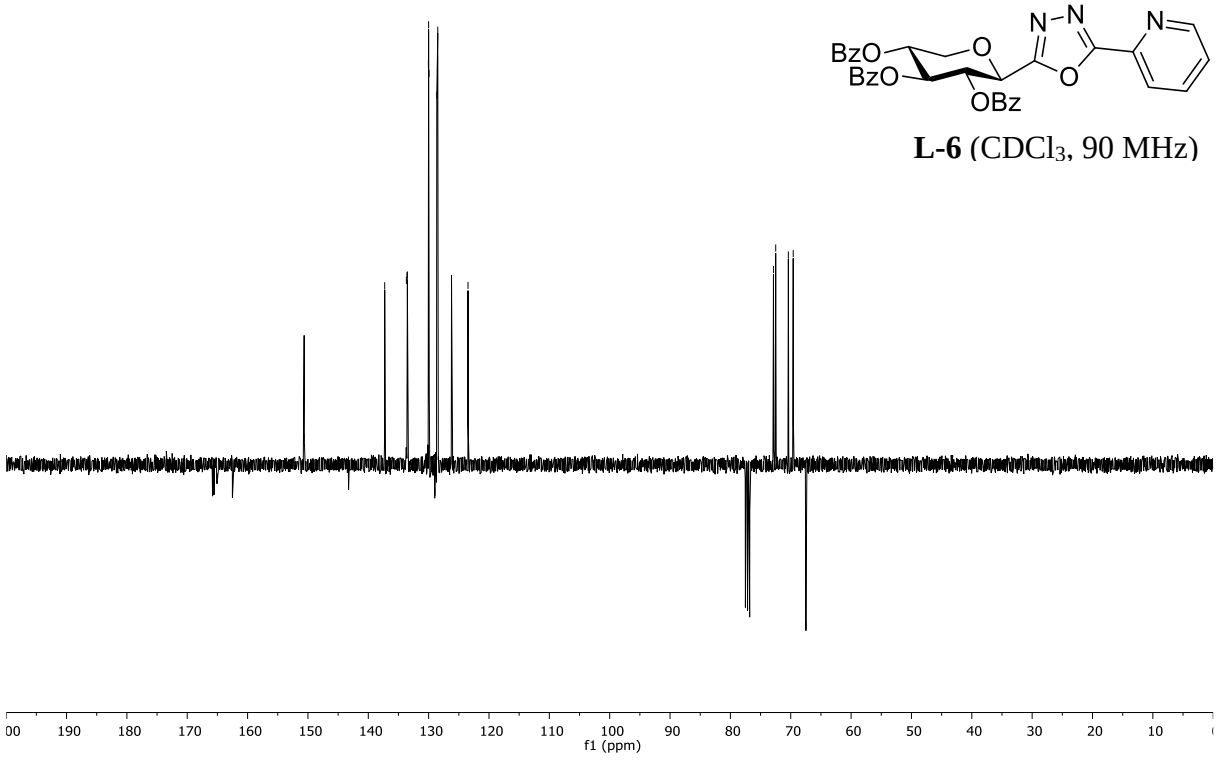

L-6 ($CDCl_3$, 90 MHz)

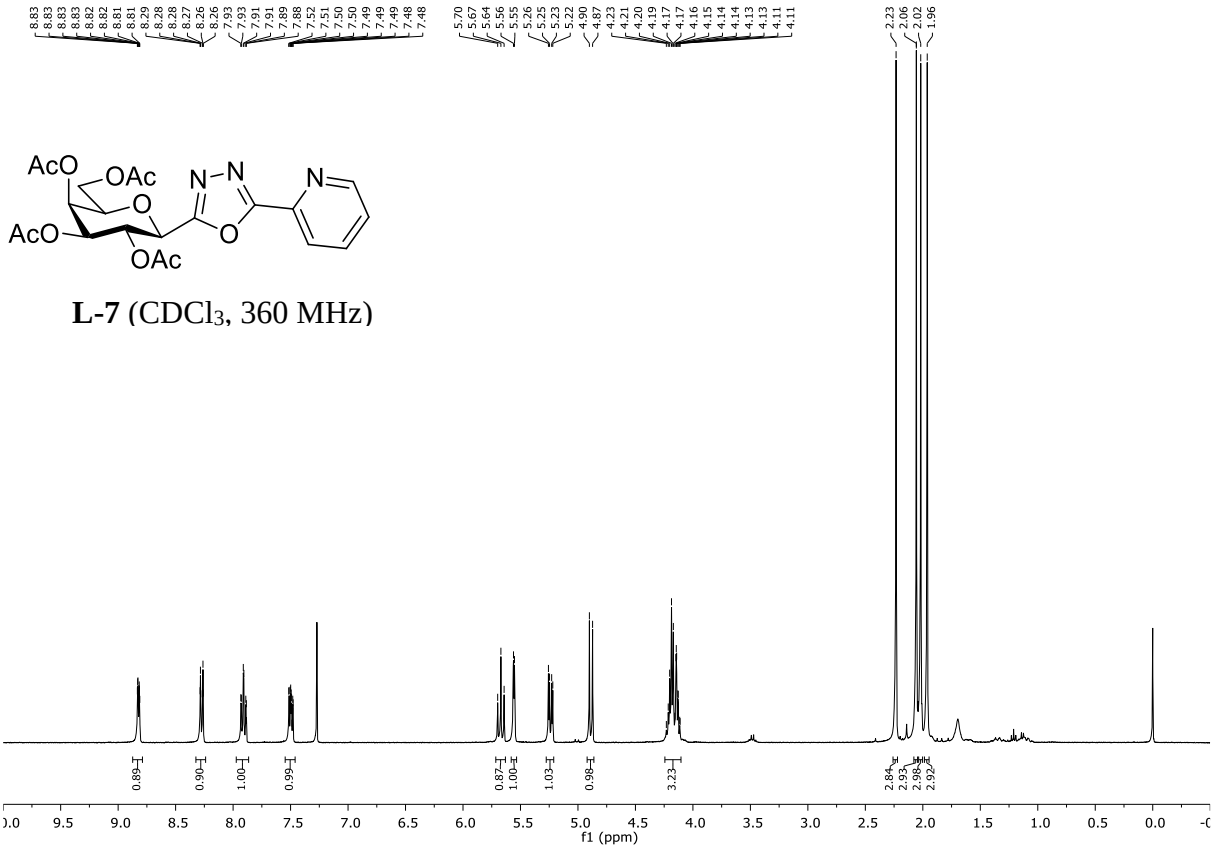

L-7 ($CDCl_3$, 360 MHz)

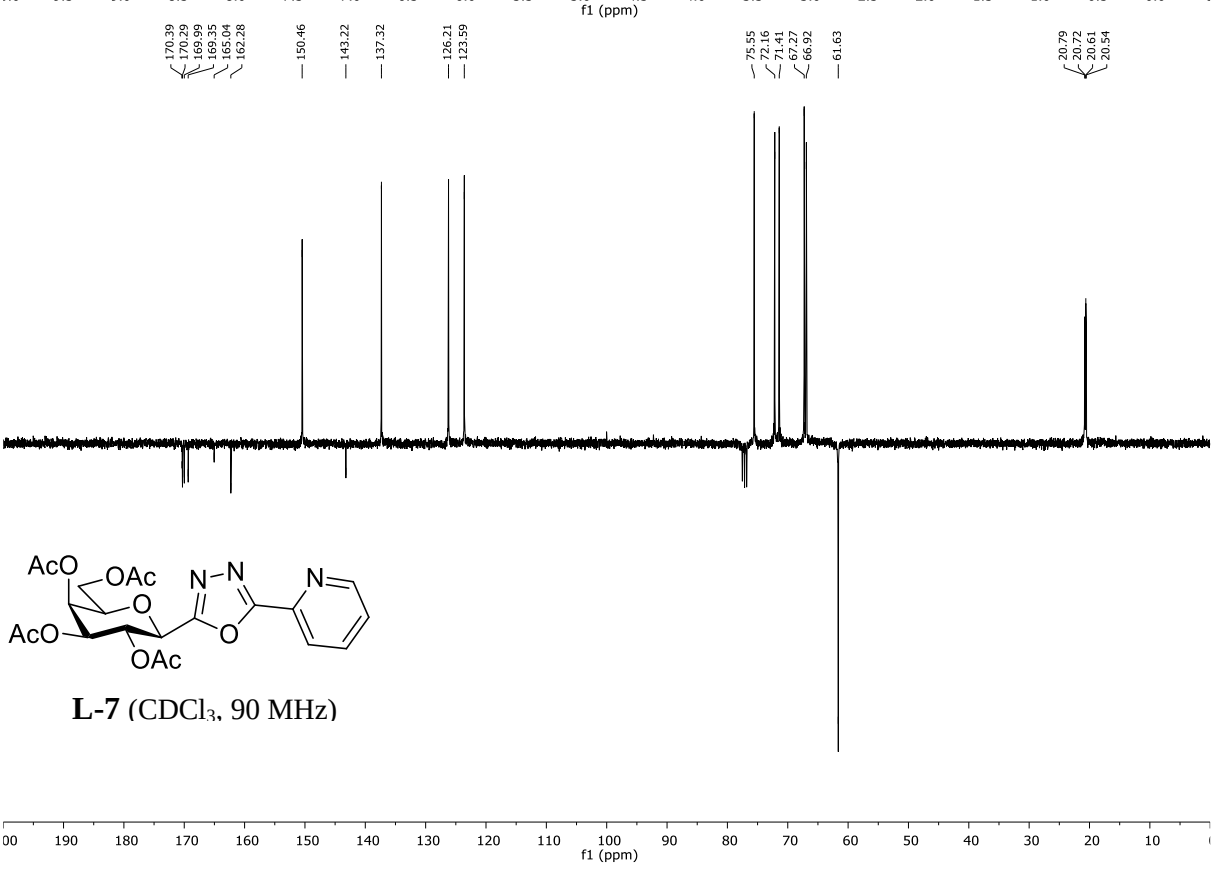

L-7 ($CDCl_3$, 90 MHz)

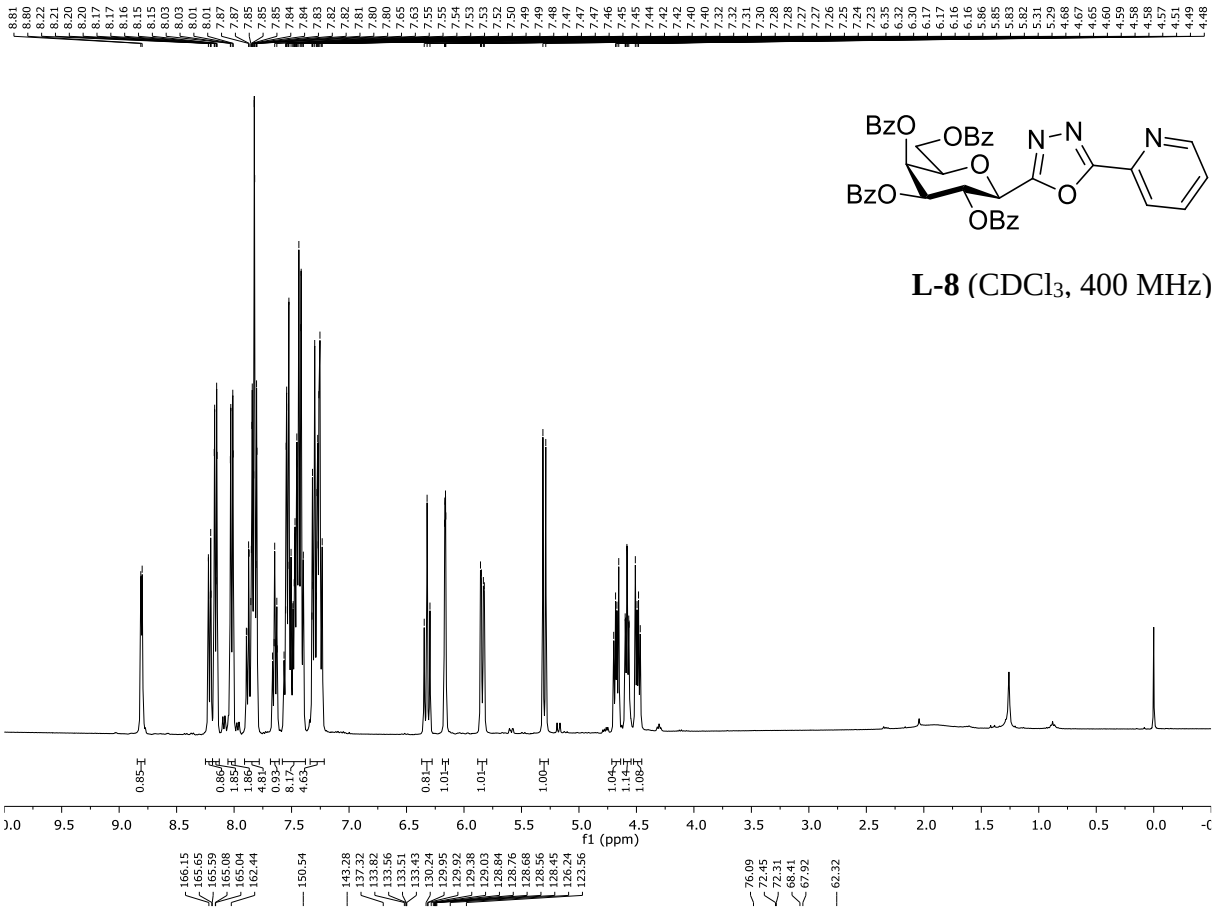

L-8 ($CDCl_3$, 400 MHz)

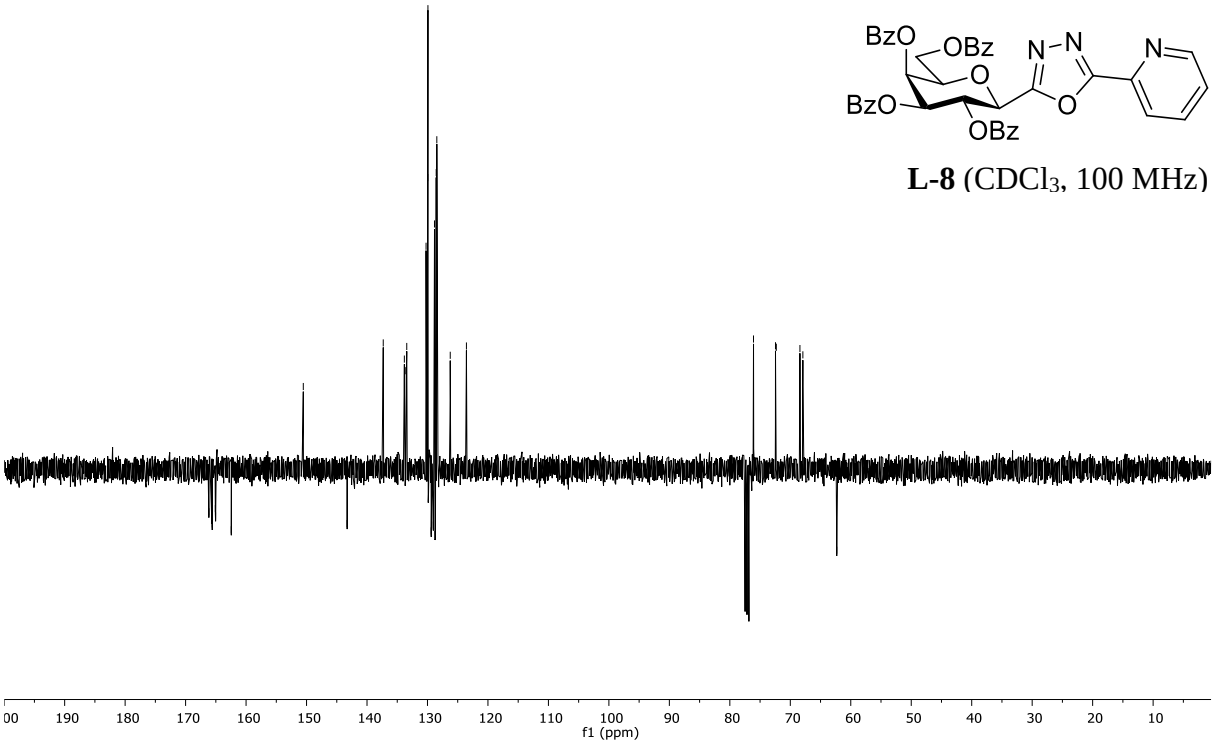

L-8 ($CDCl_3$, 100 MHz)

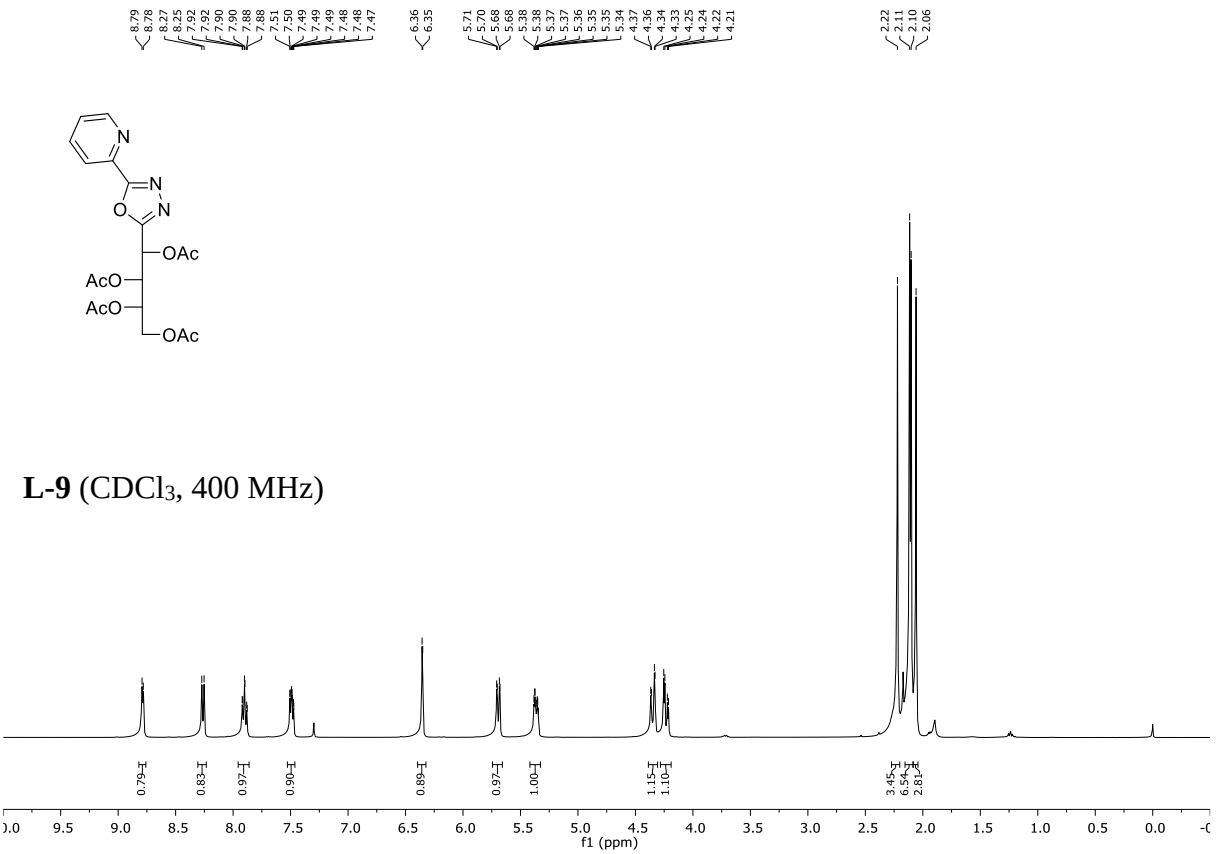

L-9 ($CDCl_3$, 400 MHz)

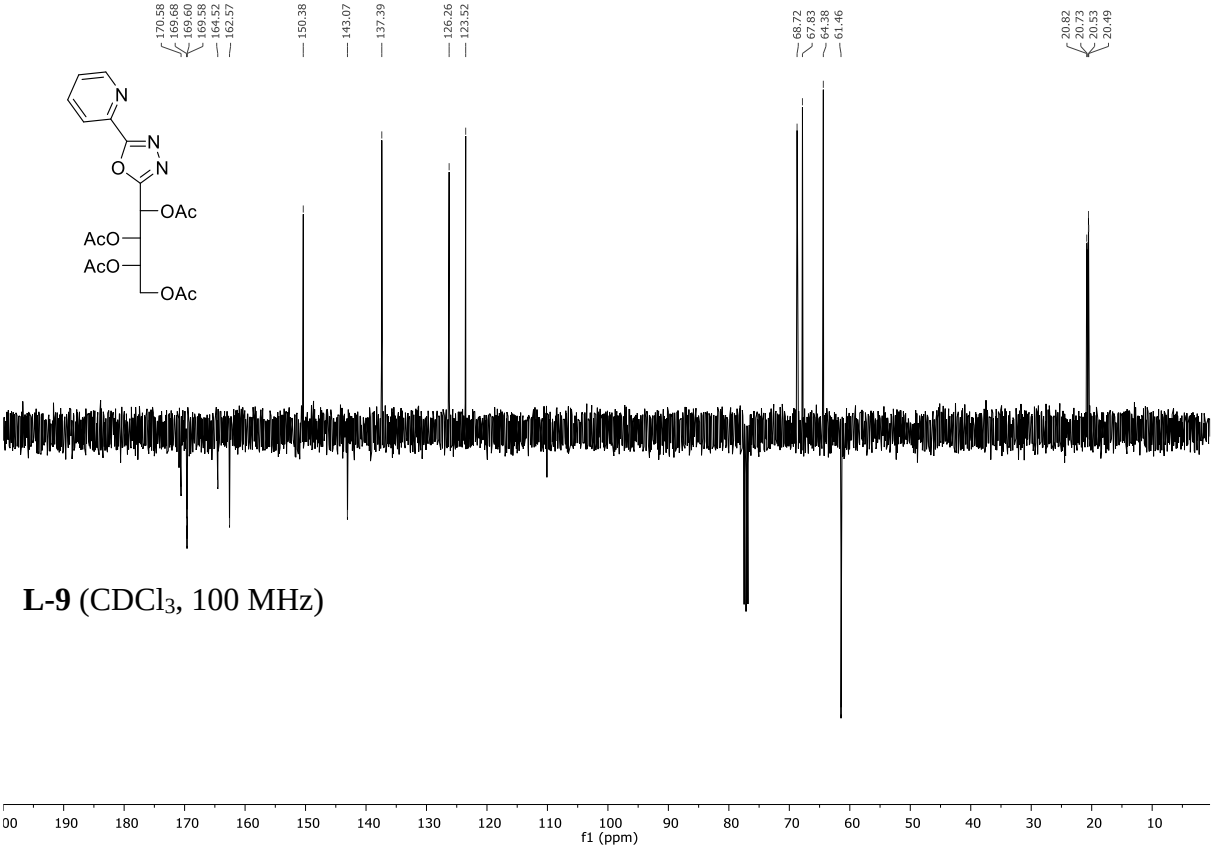

L-9 ($CDCl_3$, 100 MHz)

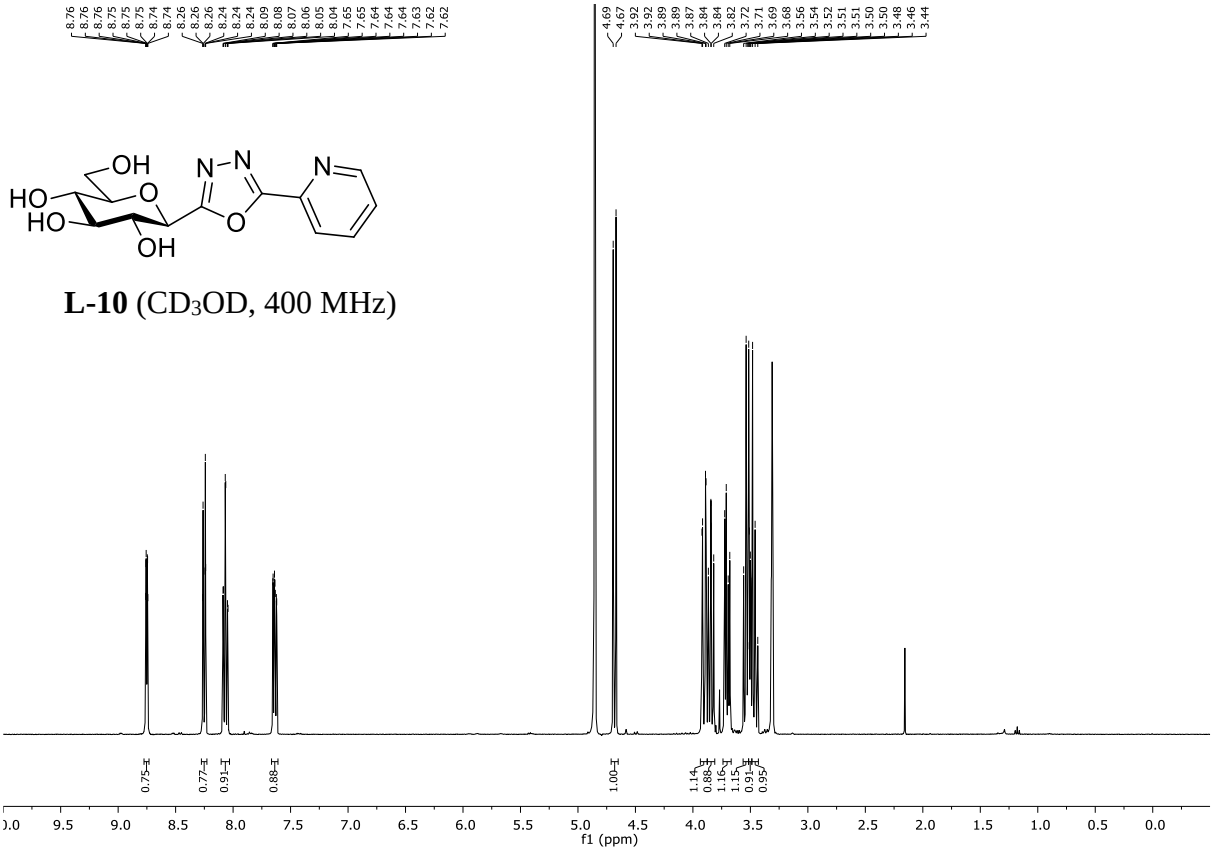

L-10 (CD_3OD, 400 MHz)

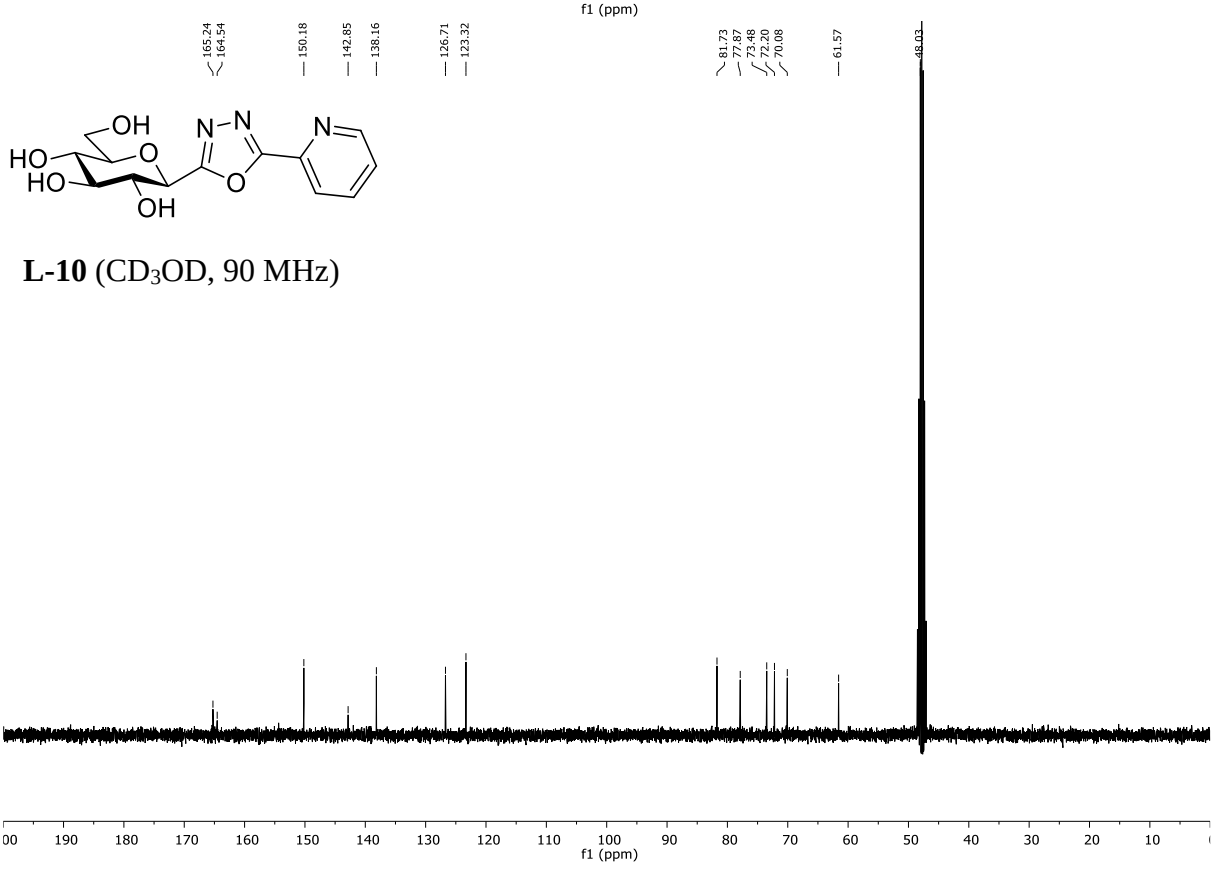

L-10 (CD_3OD, 90 MHz)

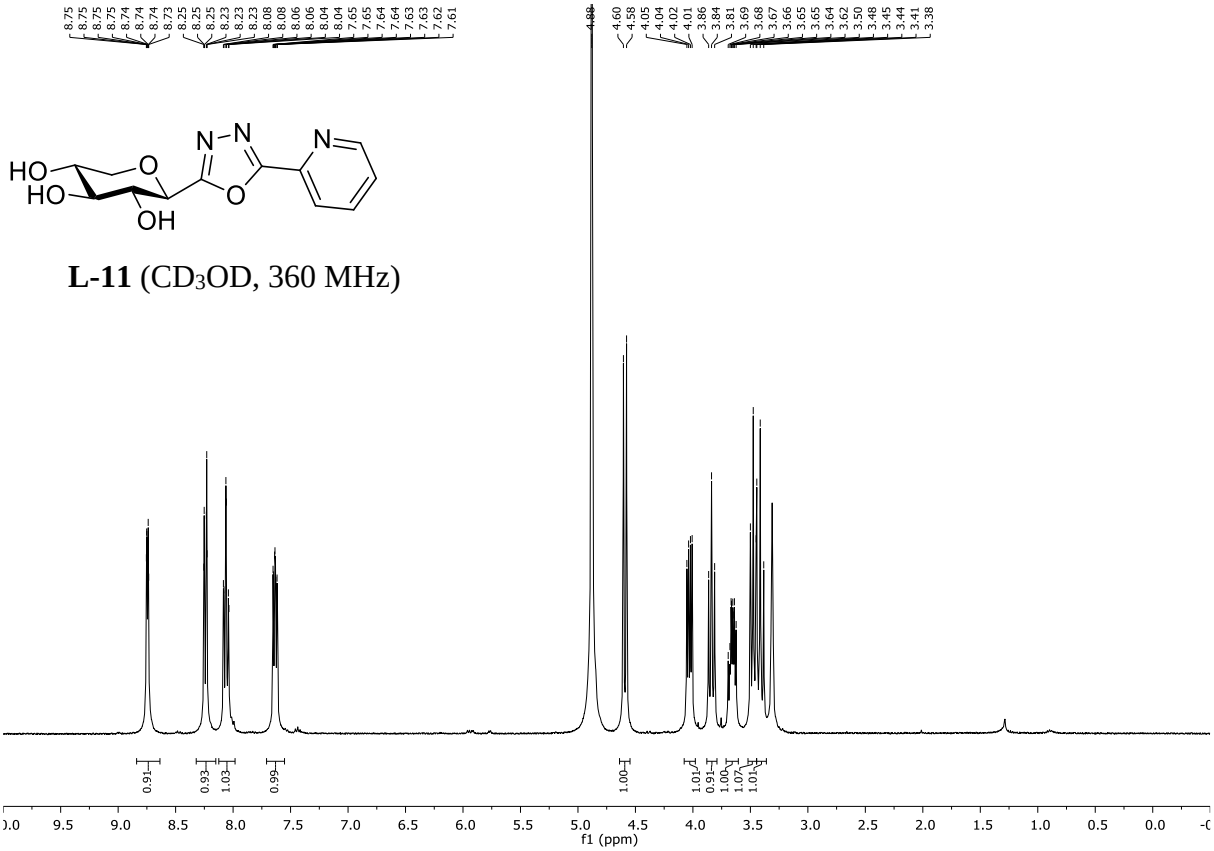

L-11 (CD_3OD, 360 MHz)

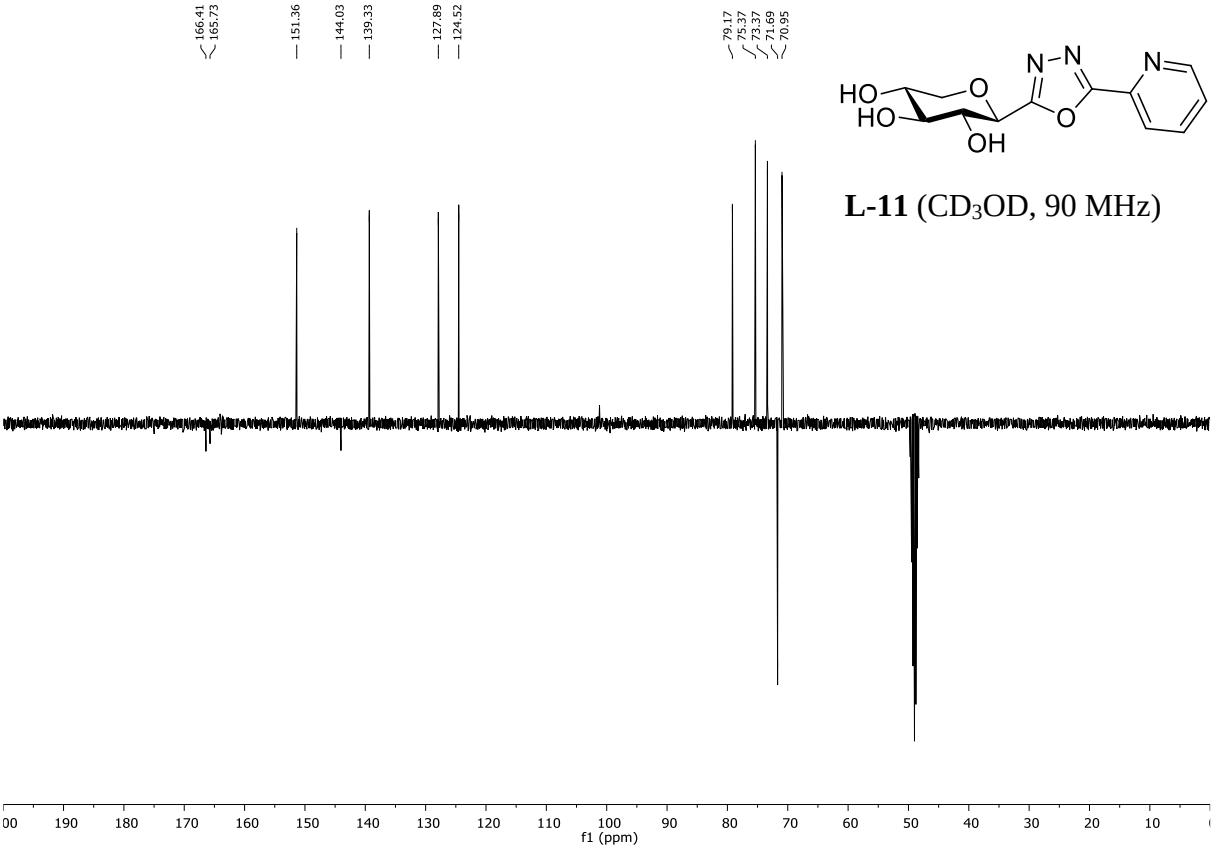

L-11 (CD_3OD, 90 MHz)

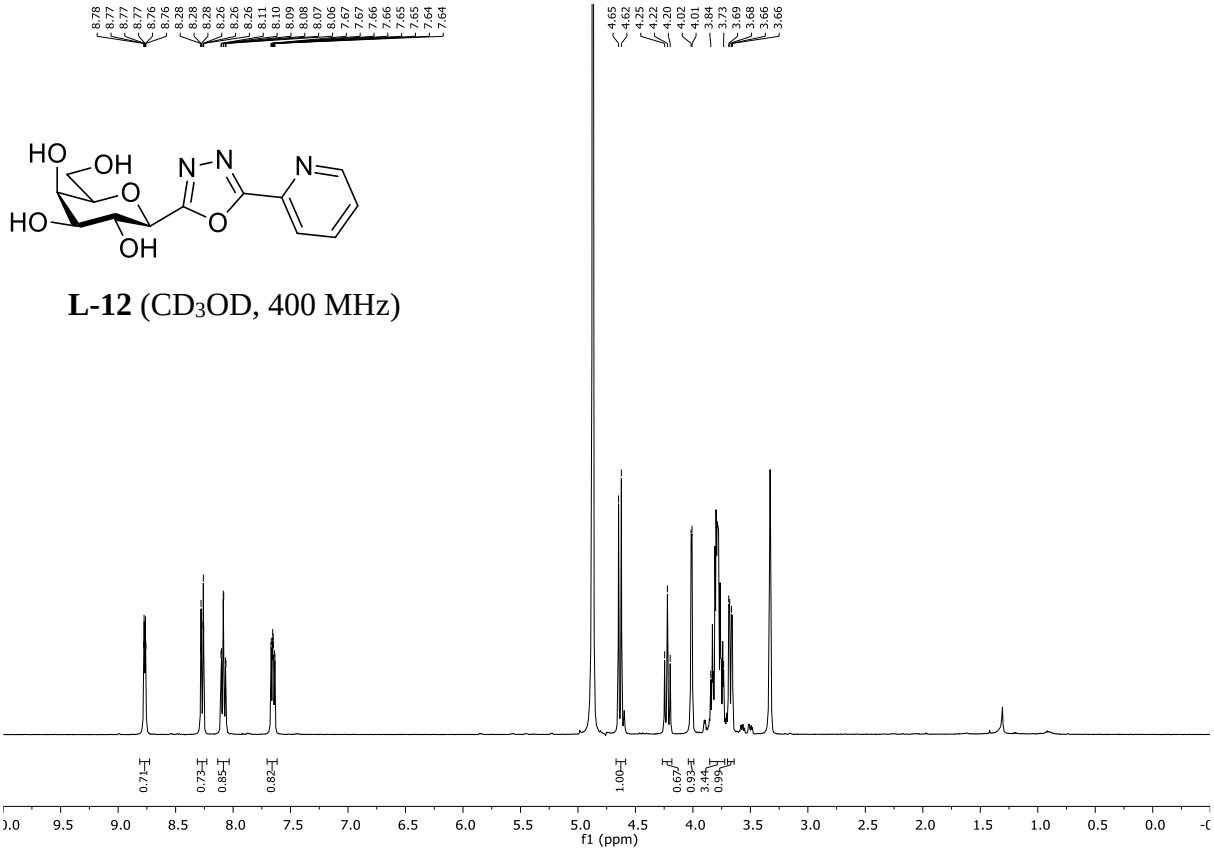

L-12 (CD_3OD, 400 MHz)

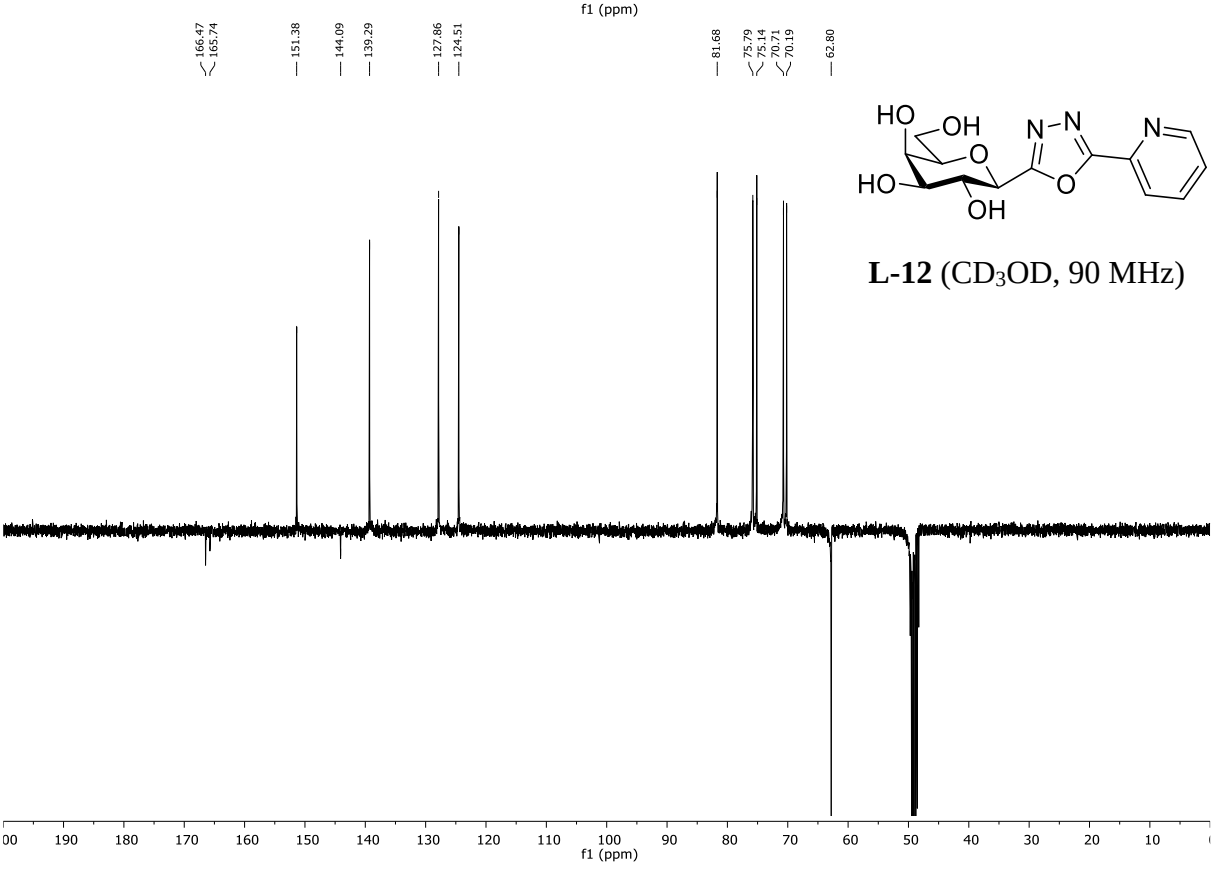

L-12 (CD_3OD, 90 MHz)

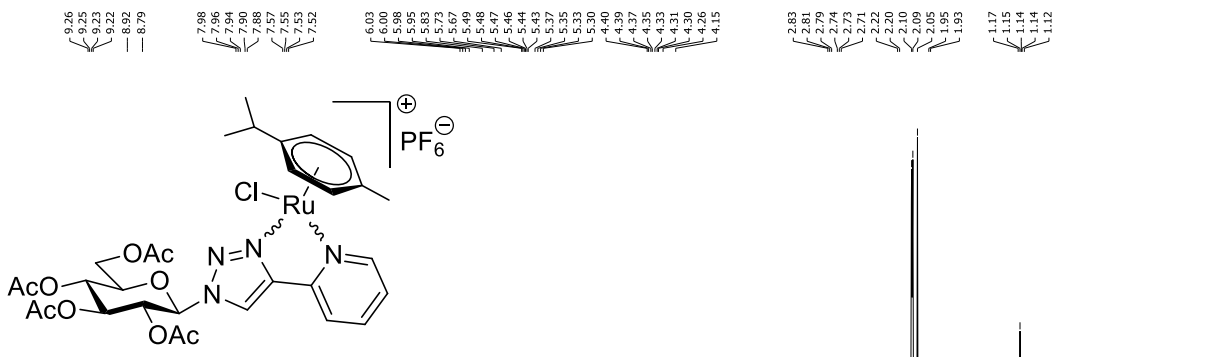

Ru-1a ($CDCl_3$, 400 MHz)

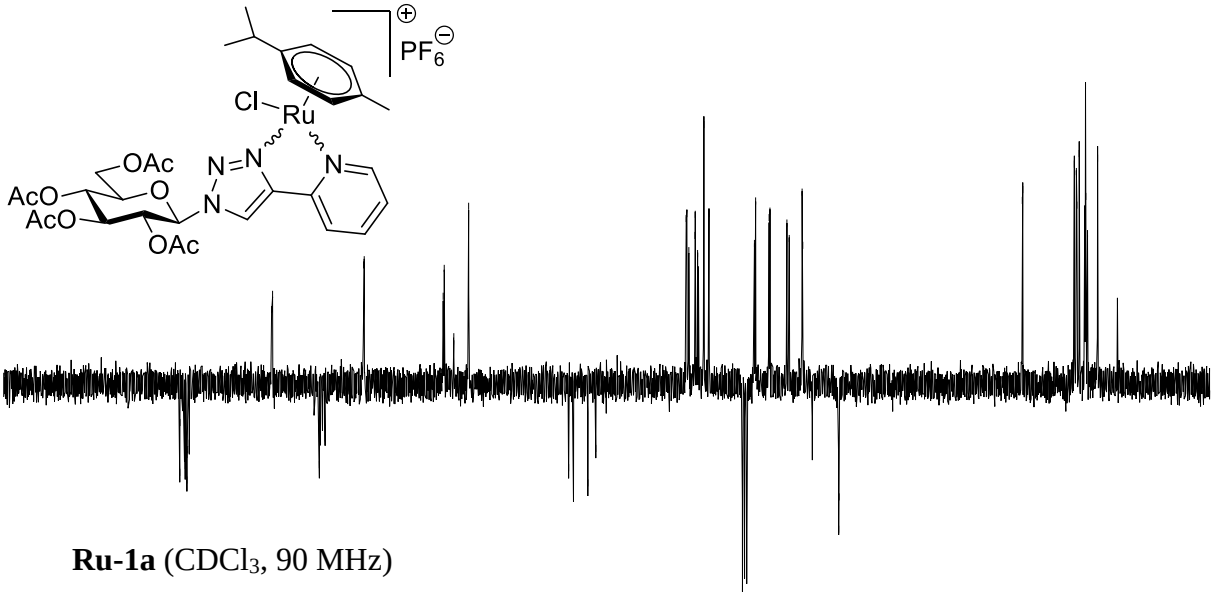

Ru-1a ($CDCl_3$, 90 MHz)

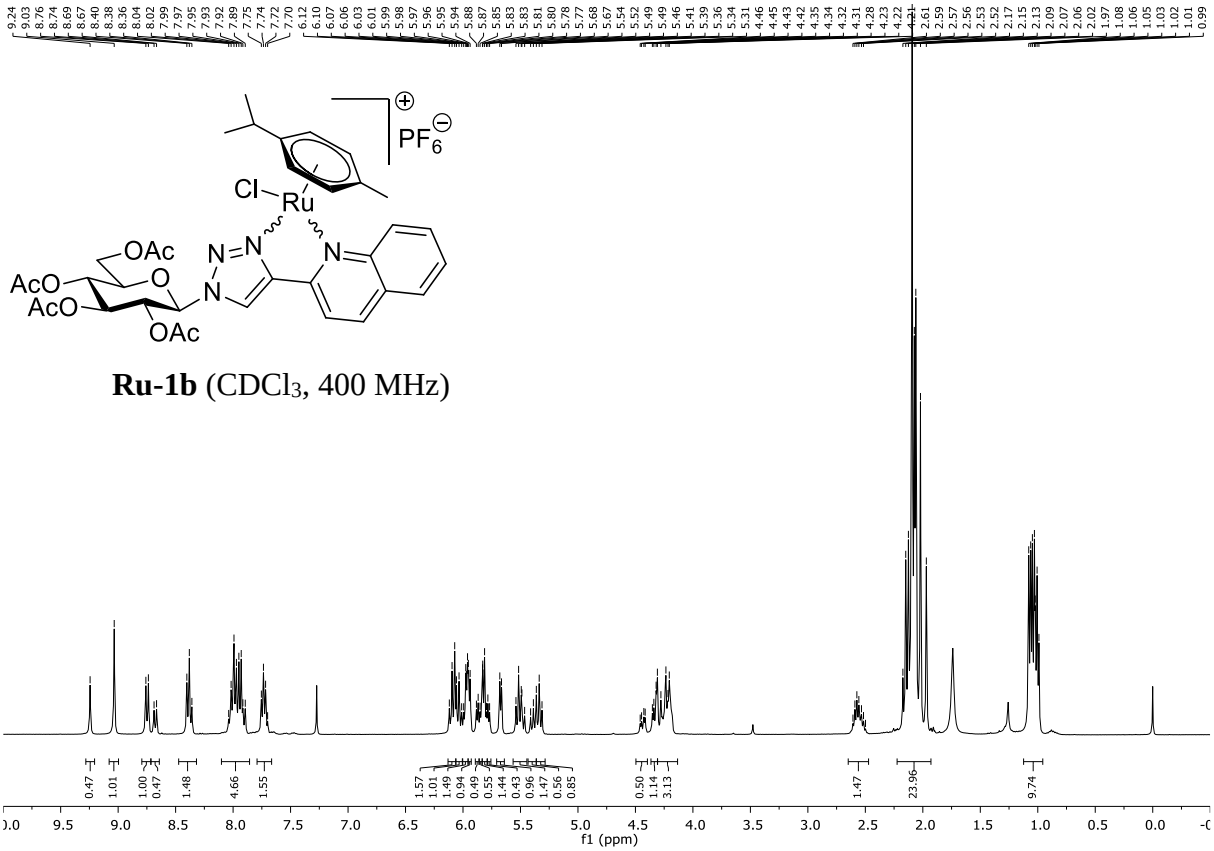

Ru-1b ($CDCl_3$, 400 MHz)

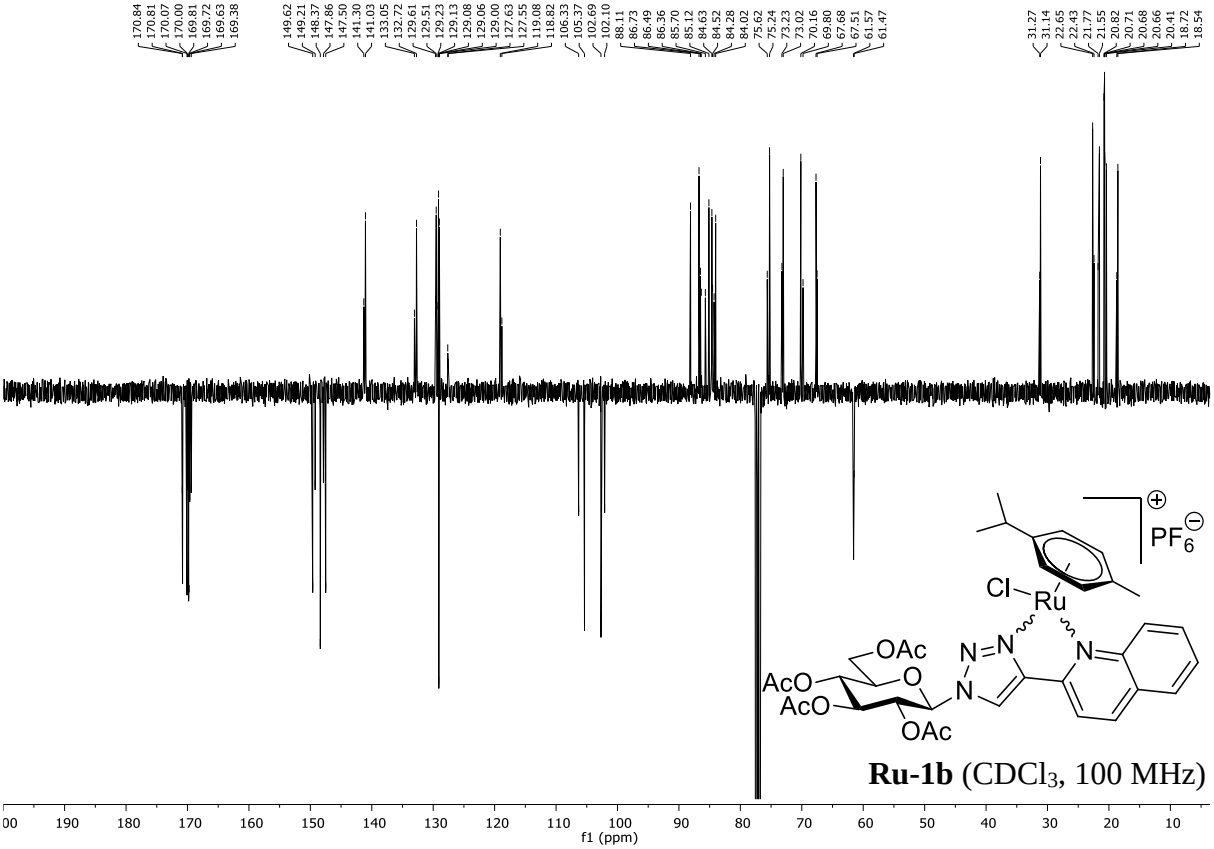

Ru-1b ($CDCl_3$, 100 MHz)

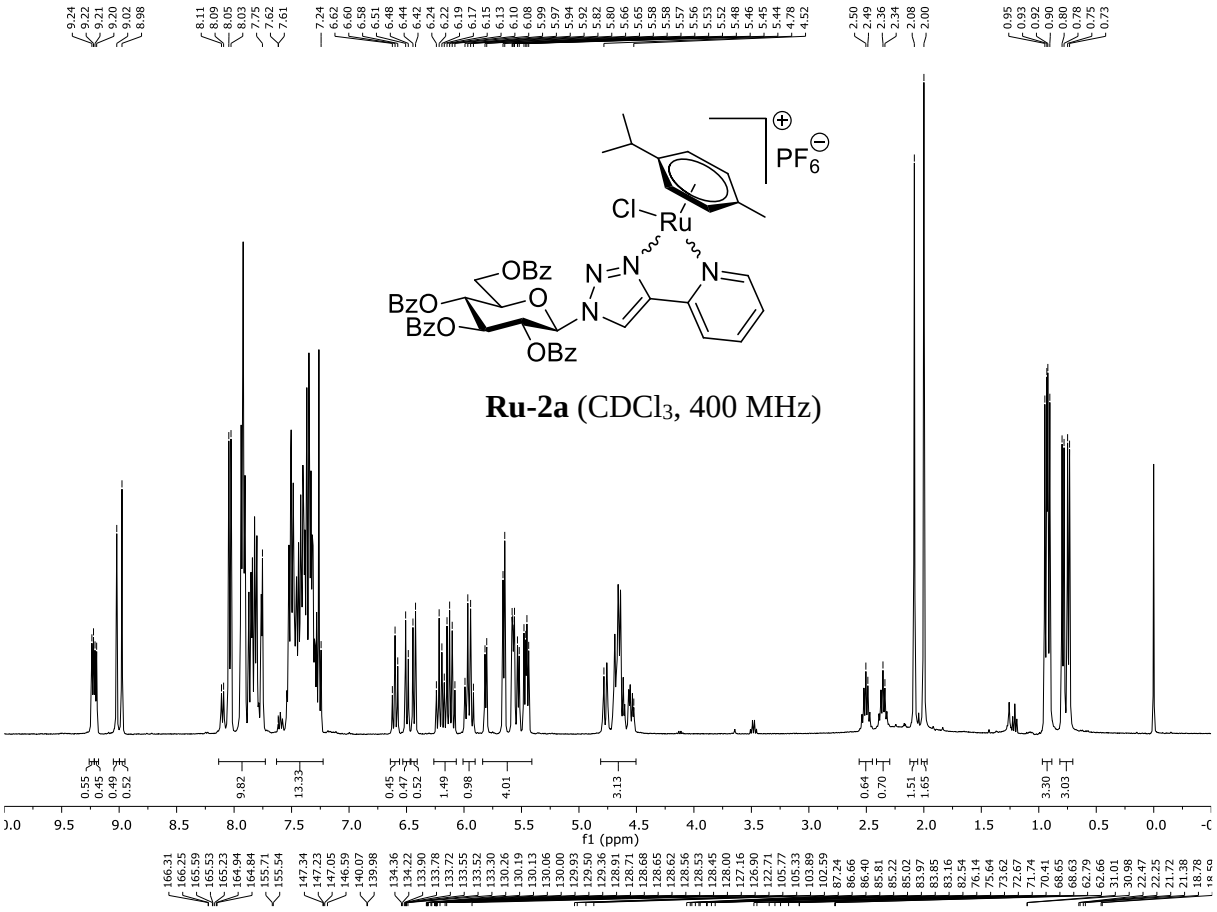

Ru-2a ($CDCl_3$, 400 MHz)

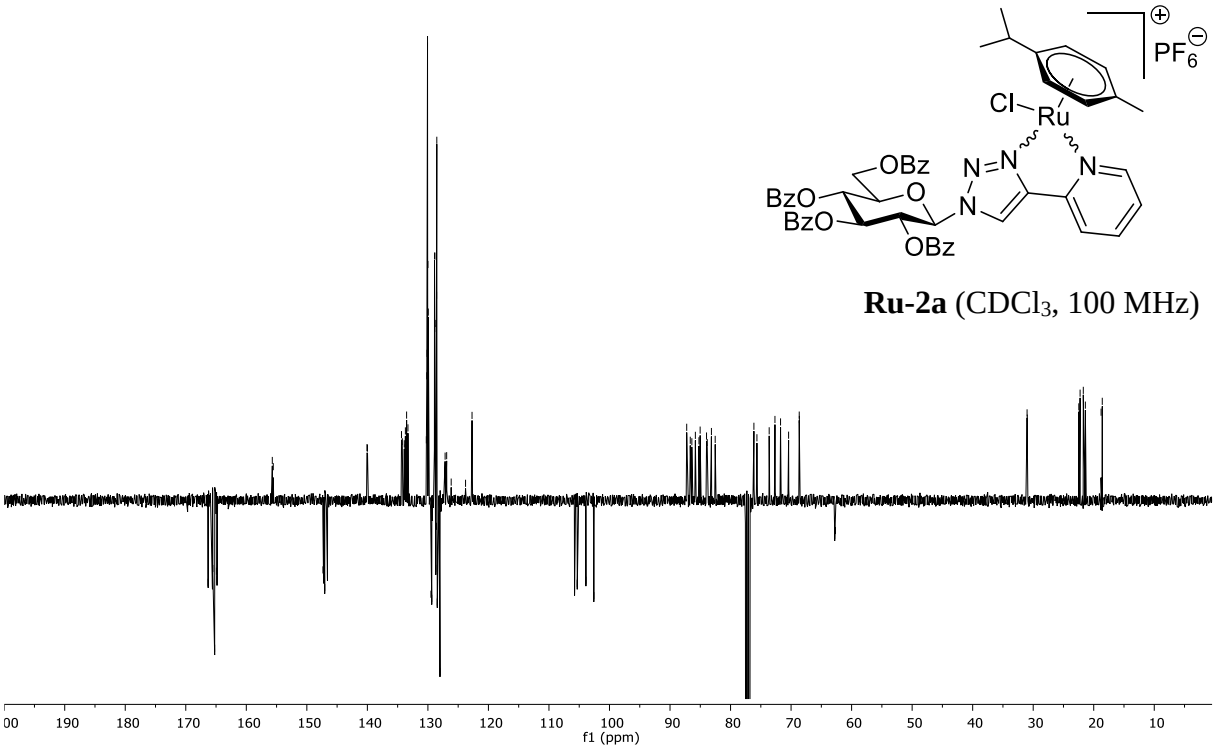

Ru-2a ($CDCl_3$, 100 MHz)

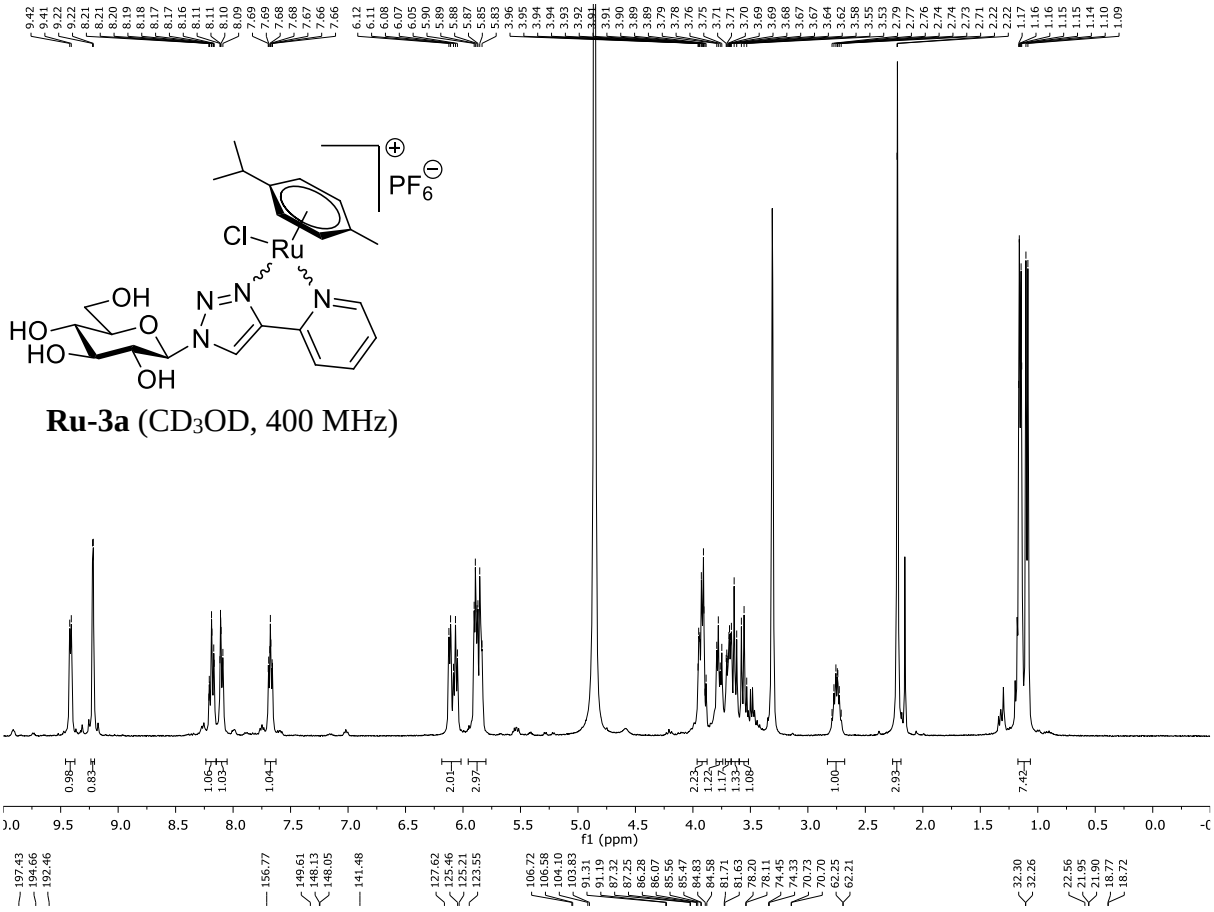

Ru-3a (CD_3OD, 400 MHz)

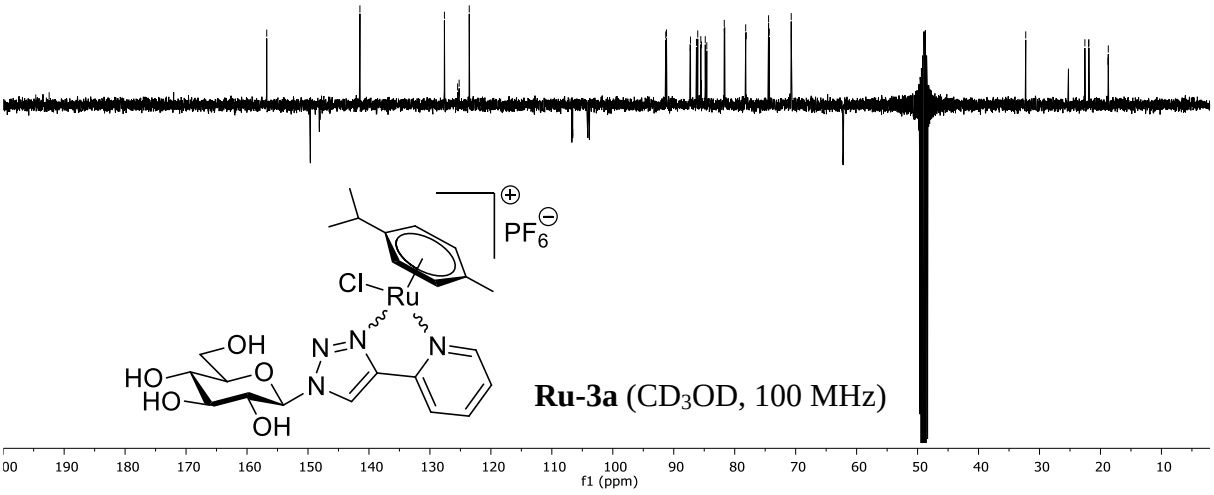

Ru-3a (CD_3OD, 100 MHz)

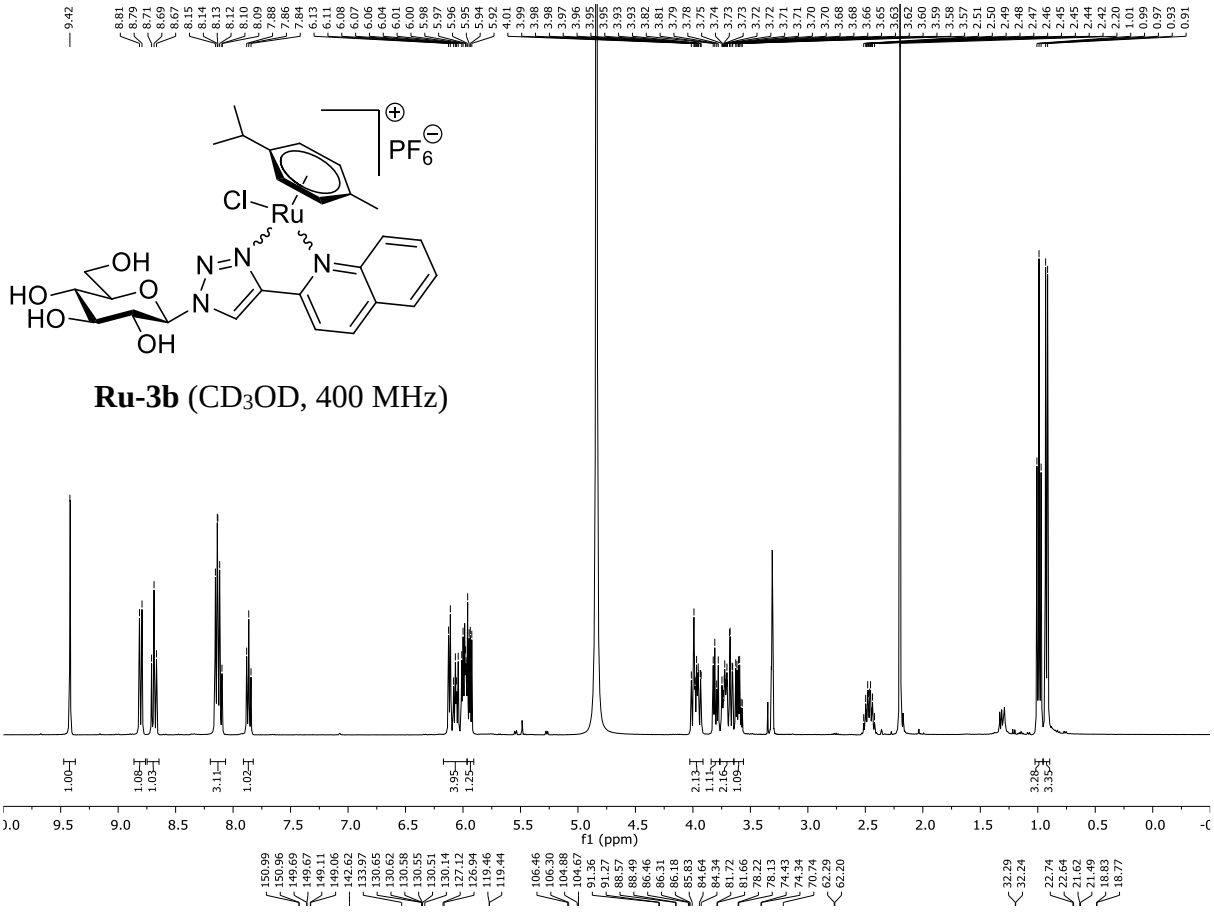

Ru-3b (CD_3OD, 400 MHz)

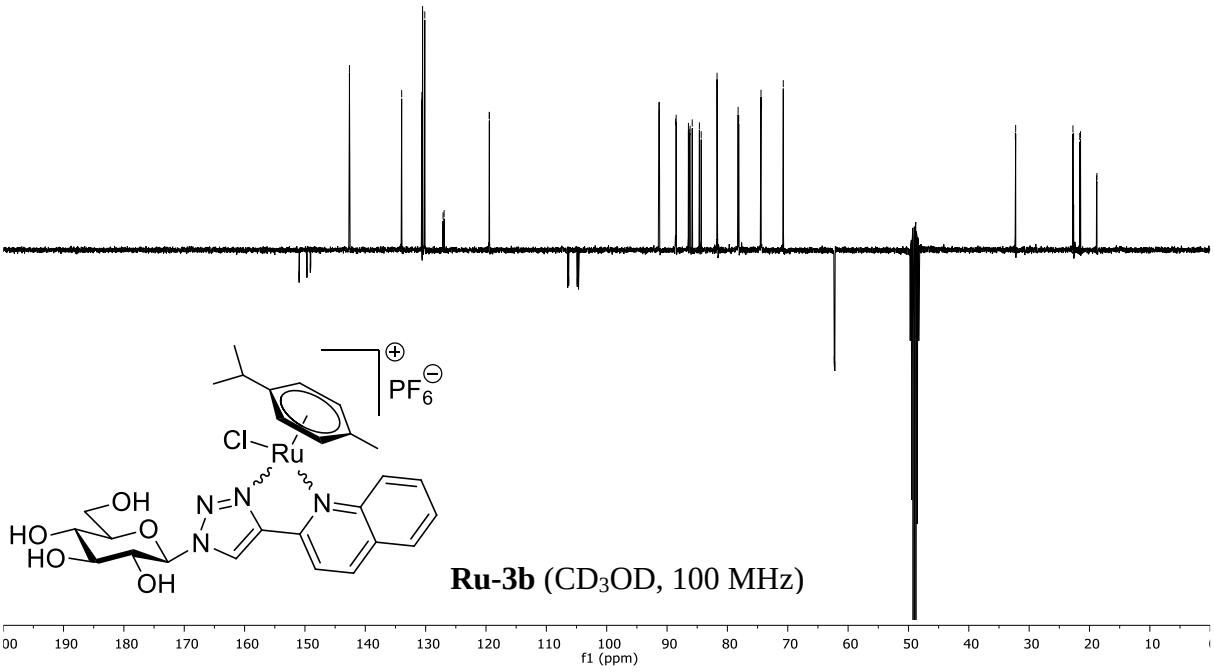

Ru-3b (CD_3OD, 100 MHz)

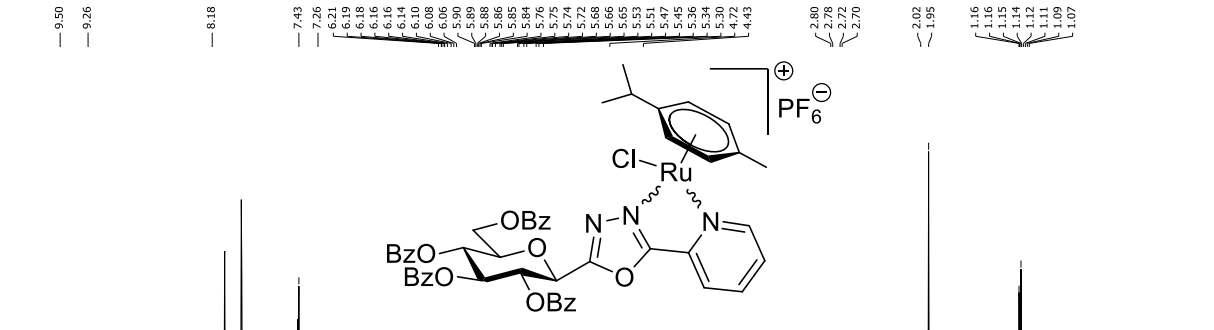

Ru-4 ($CDCl_3$, 400 MHz)

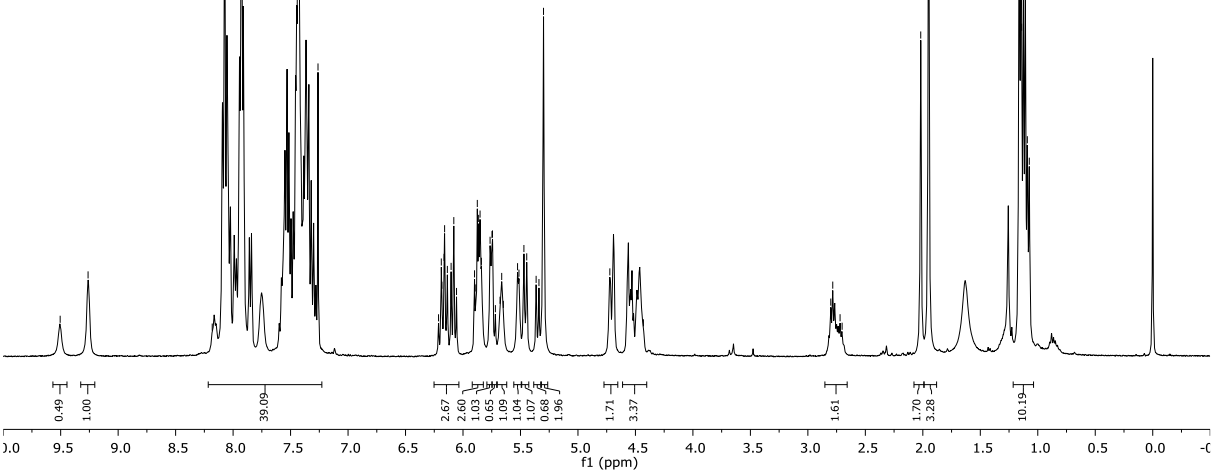

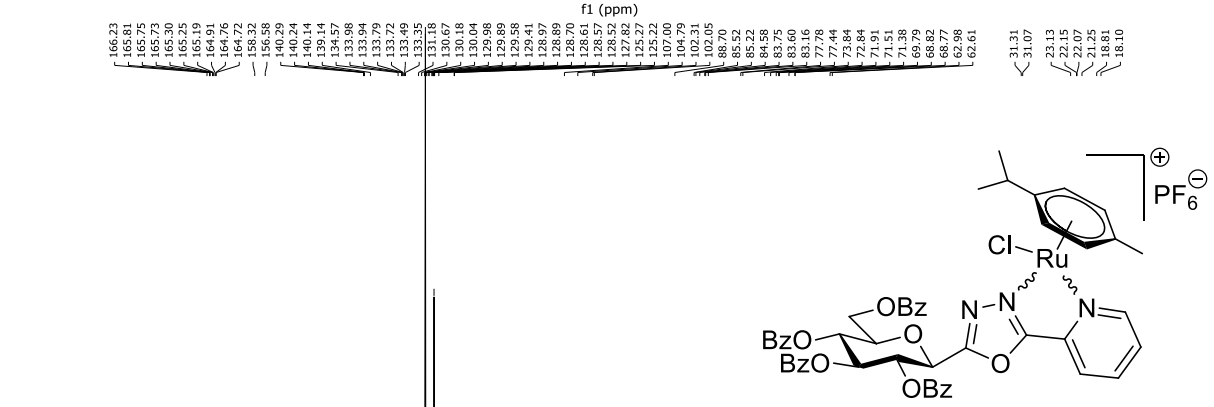

Ru-4 ($CDCl_3$, 90 MHz)

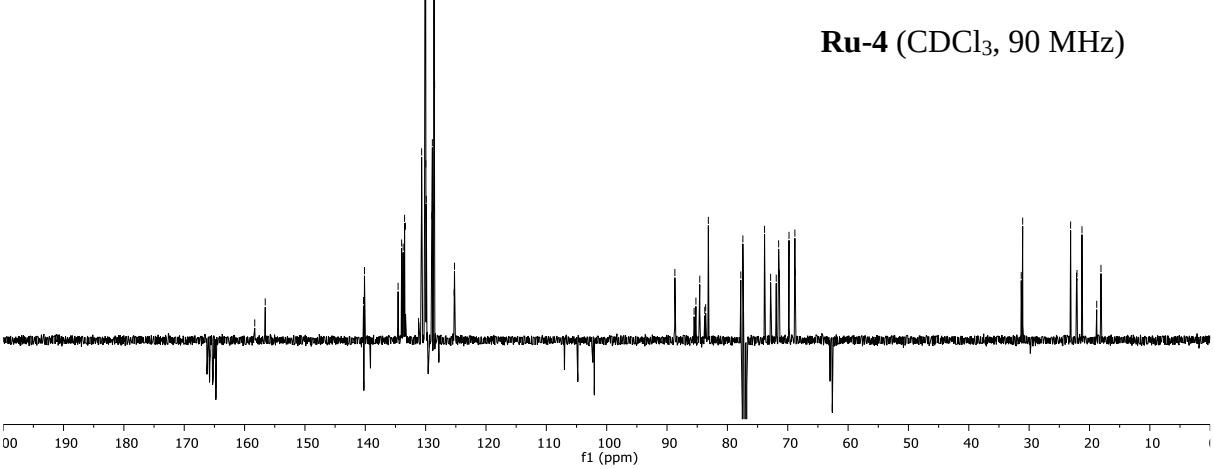

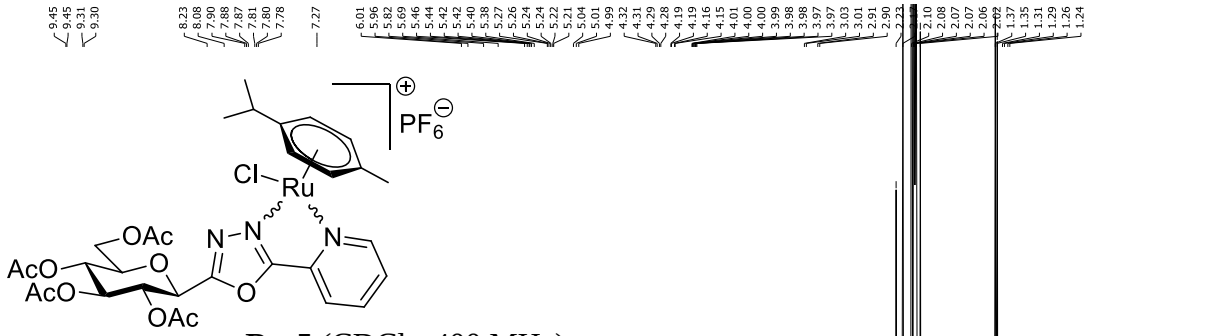

Ru-5 ($CDCl_3$, 400 MHz)

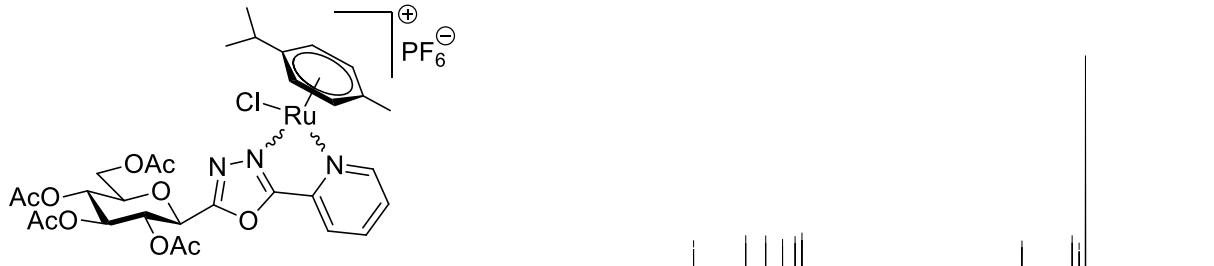

Ru-5 ($CDCl_3$, 90 MHz)

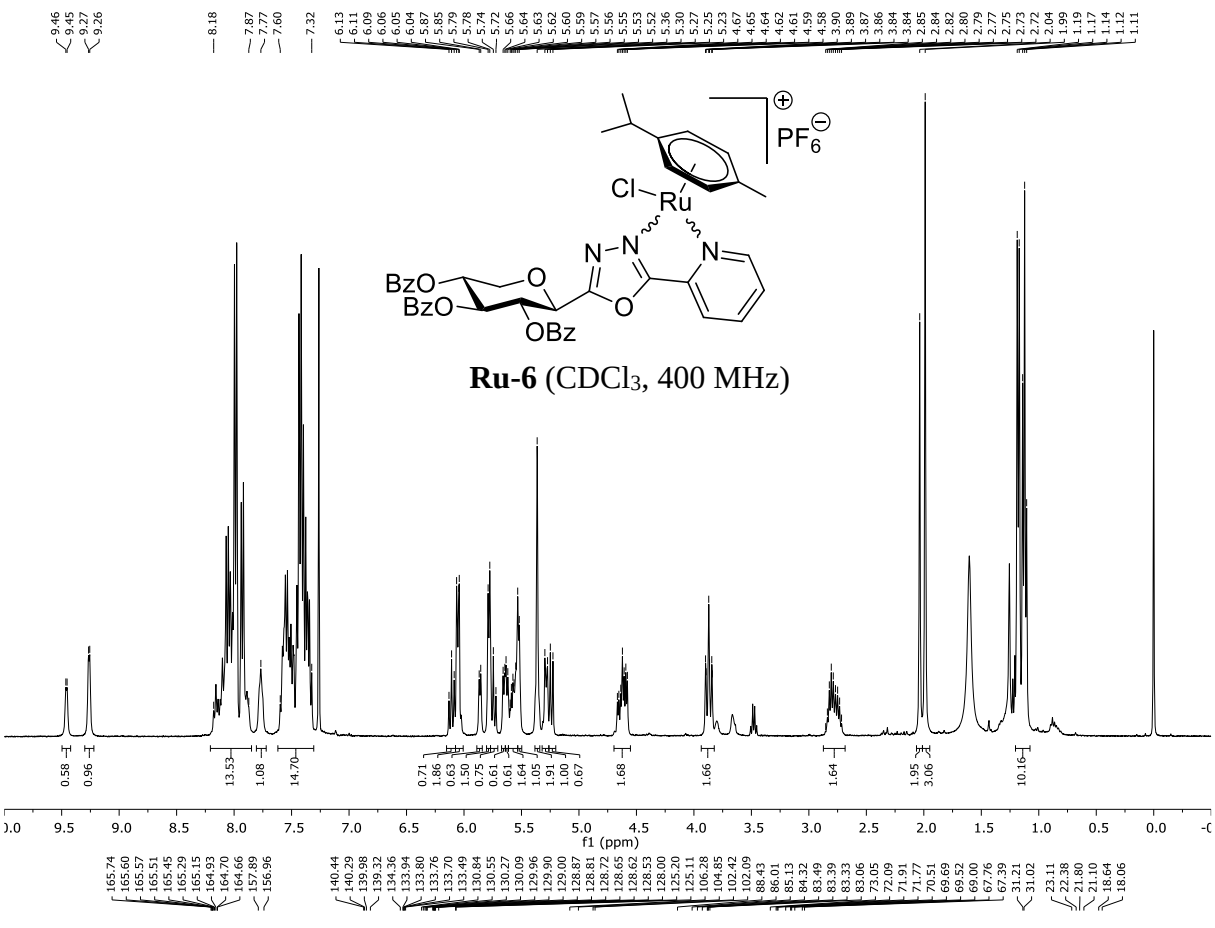

Ru-6 ($CDCl_3$, 400 MHz)

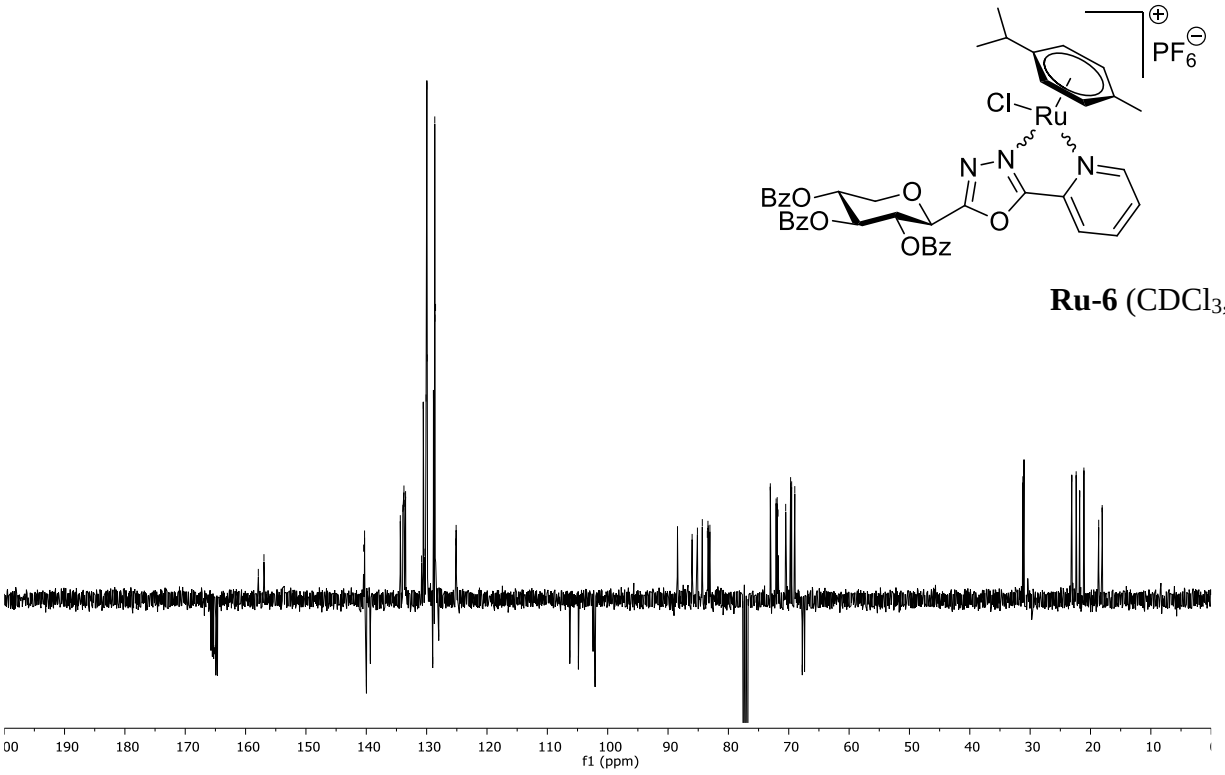

Ru-6 ($CDCl_3$, 90 MHz)

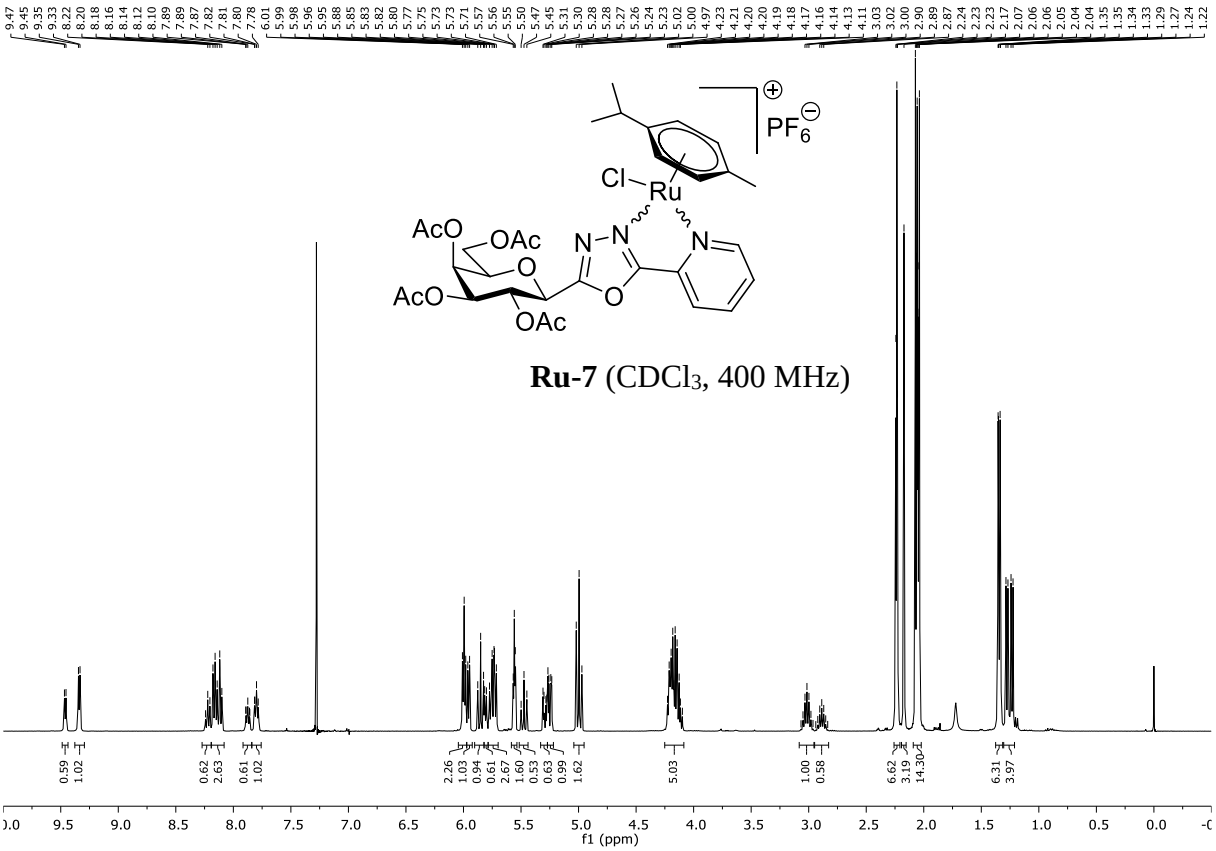

Ru-7 ($CDCl_3$, 400 MHz)

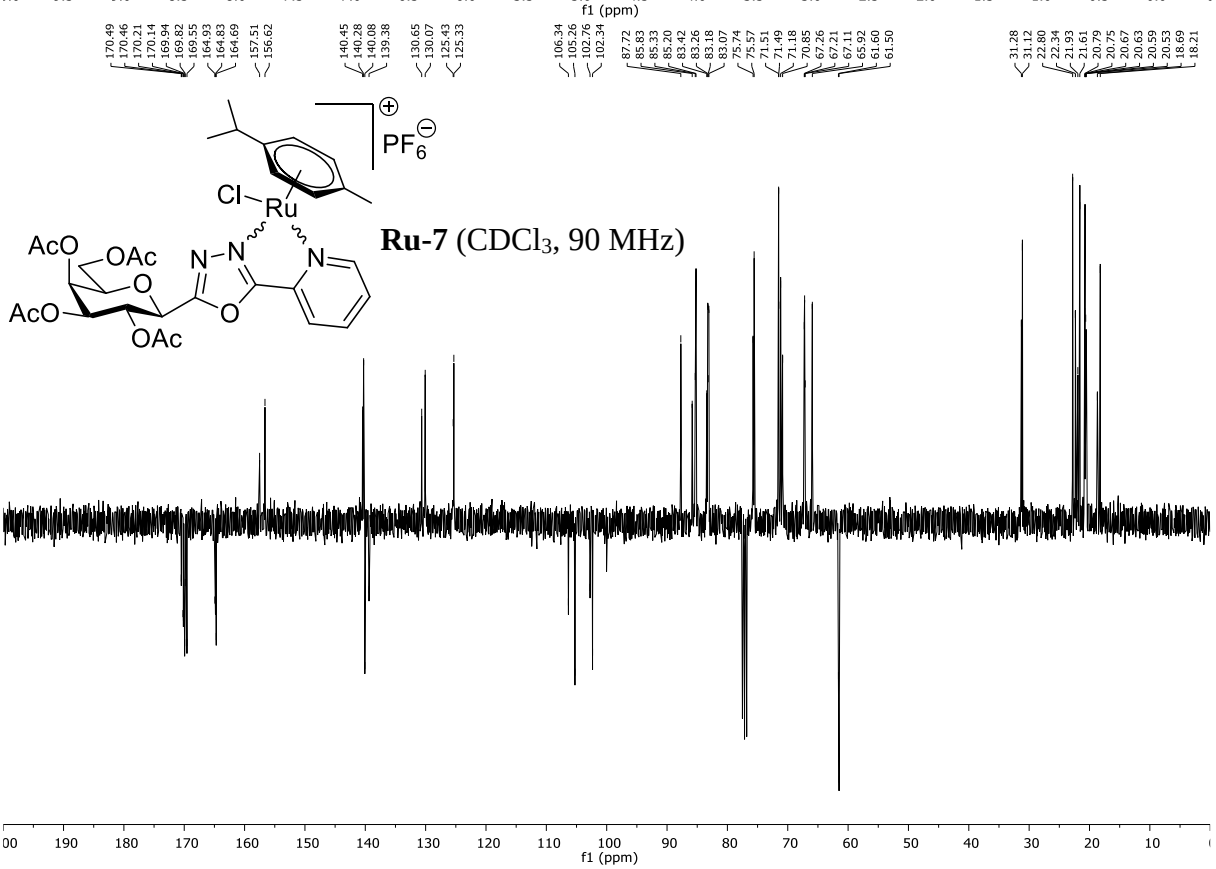

Ru-7 ($CDCl_3$, 90 MHz)

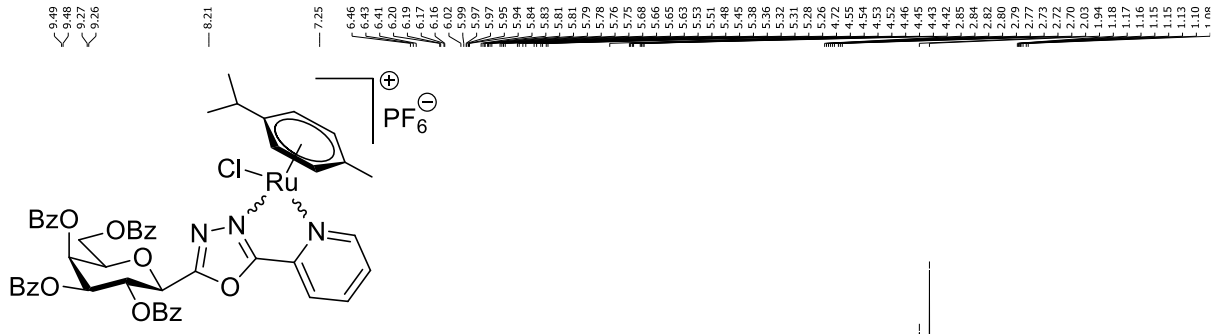

Ru-8 ($CDCl_3$, 400 MHz)

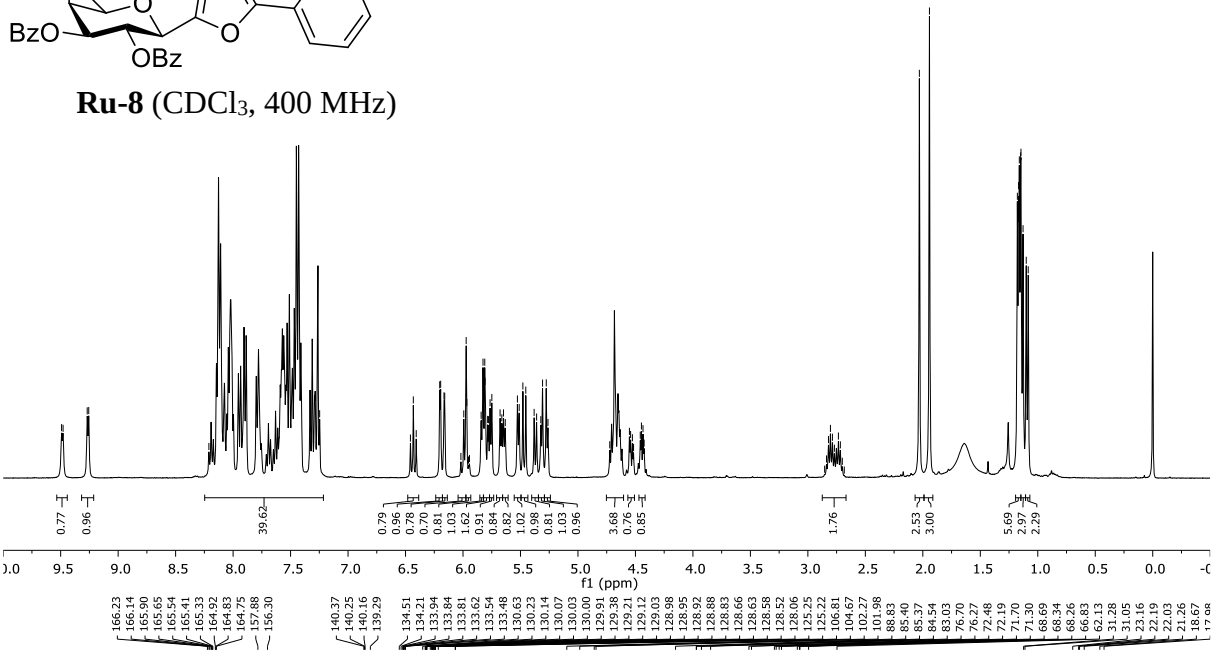

Ru-8 ($CDCl_3$, 100 MHz)

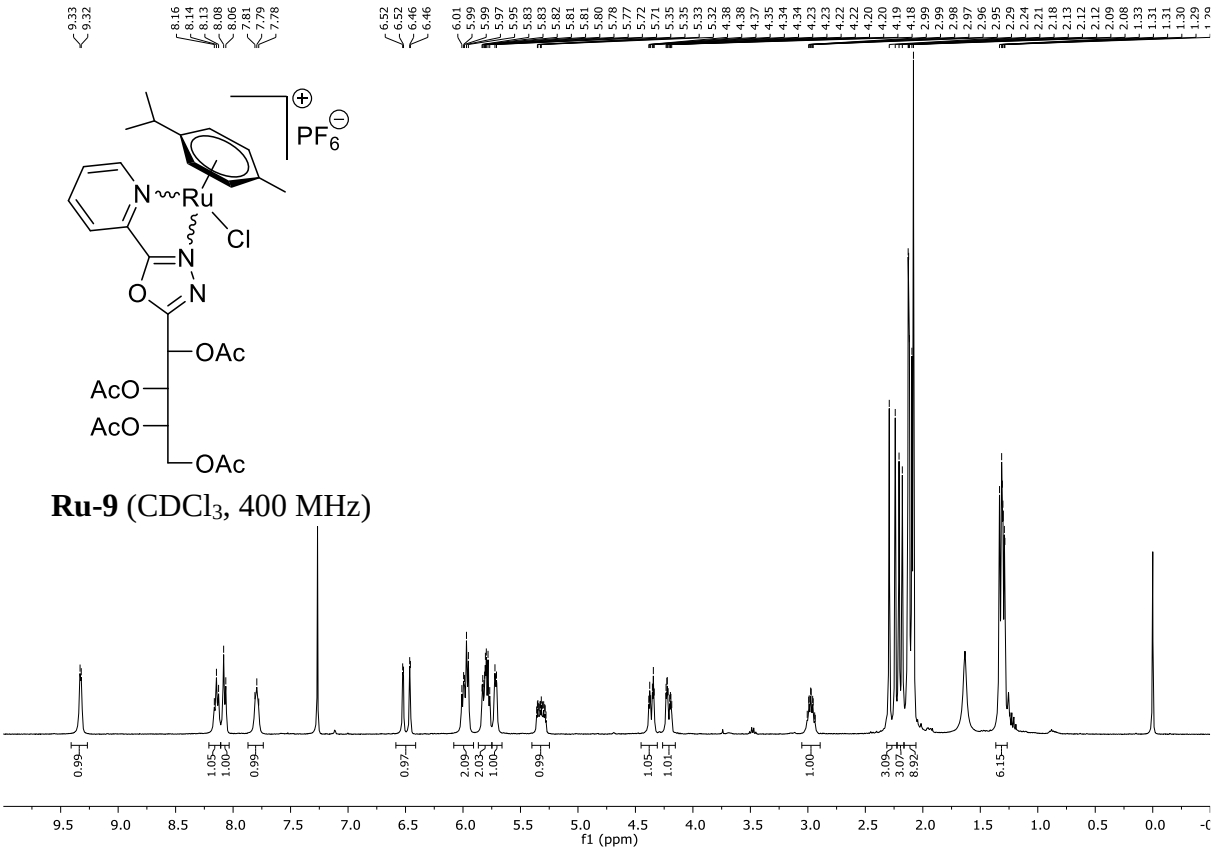

Ru-9 ($CDCl_3$, 400 MHz)

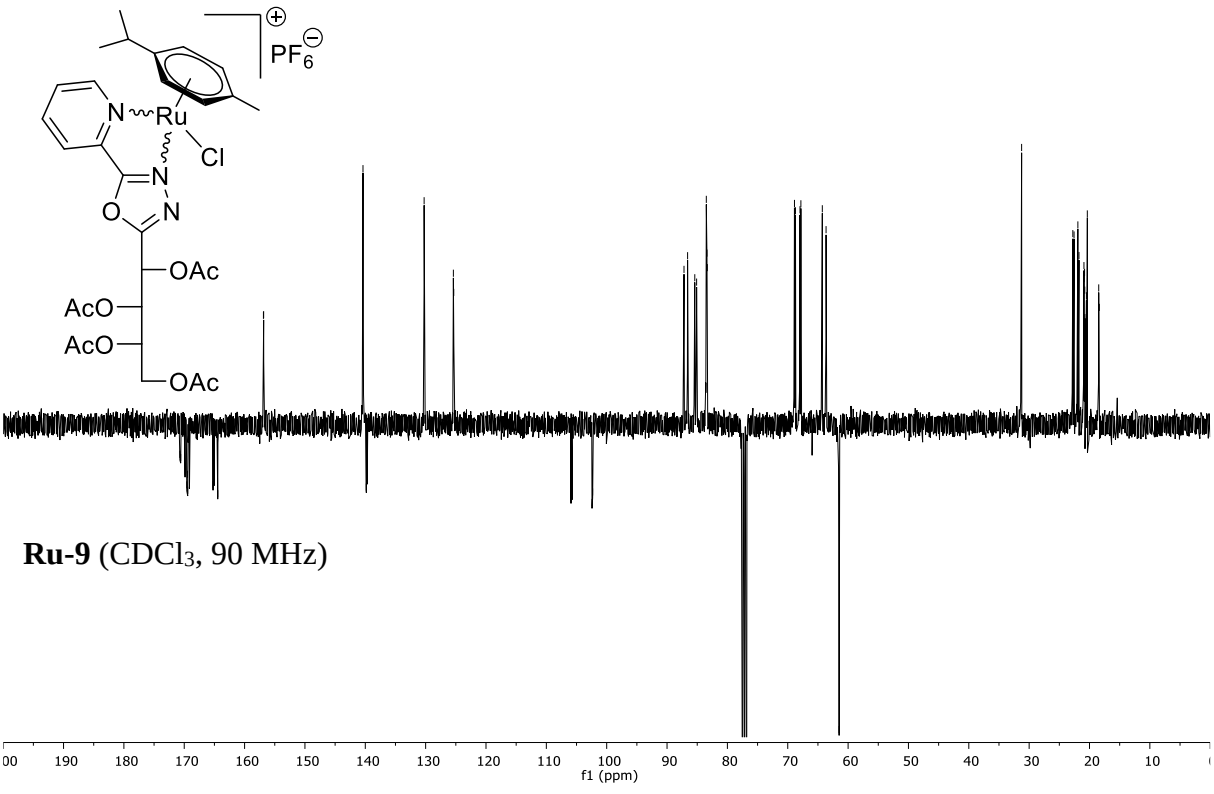

Ru-9 ($CDCl_3$, 90 MHz)

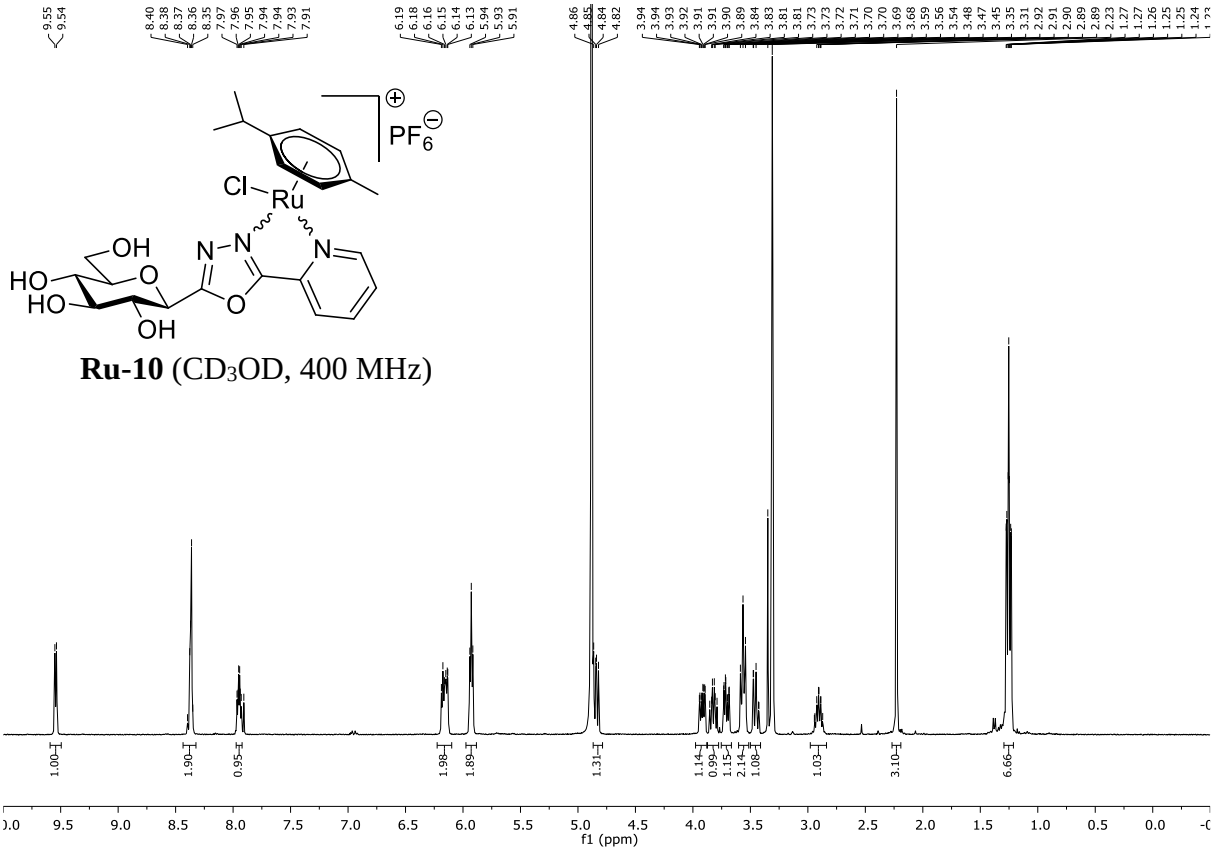

Ru-10 (CD_3OD, 400 MHz)

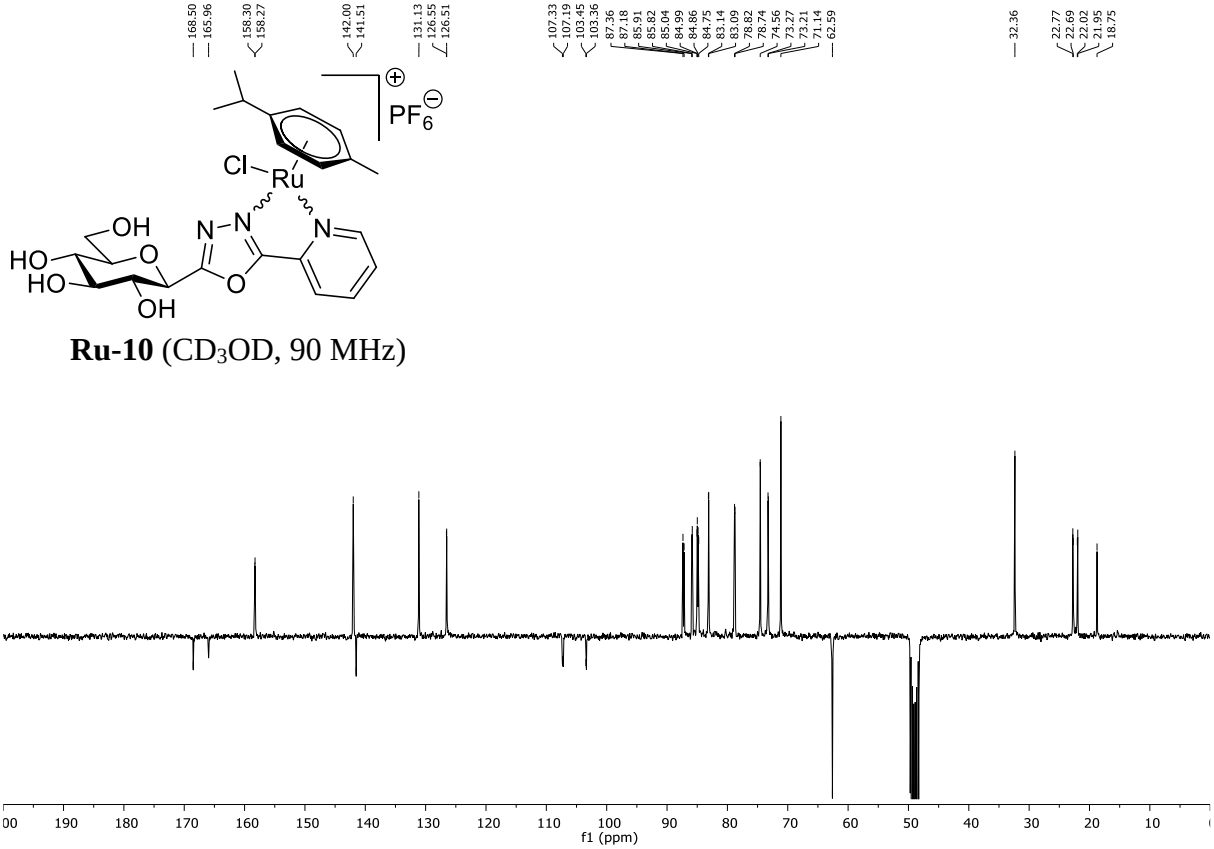

Ru-10 (CD_3OD, 90 MHz)

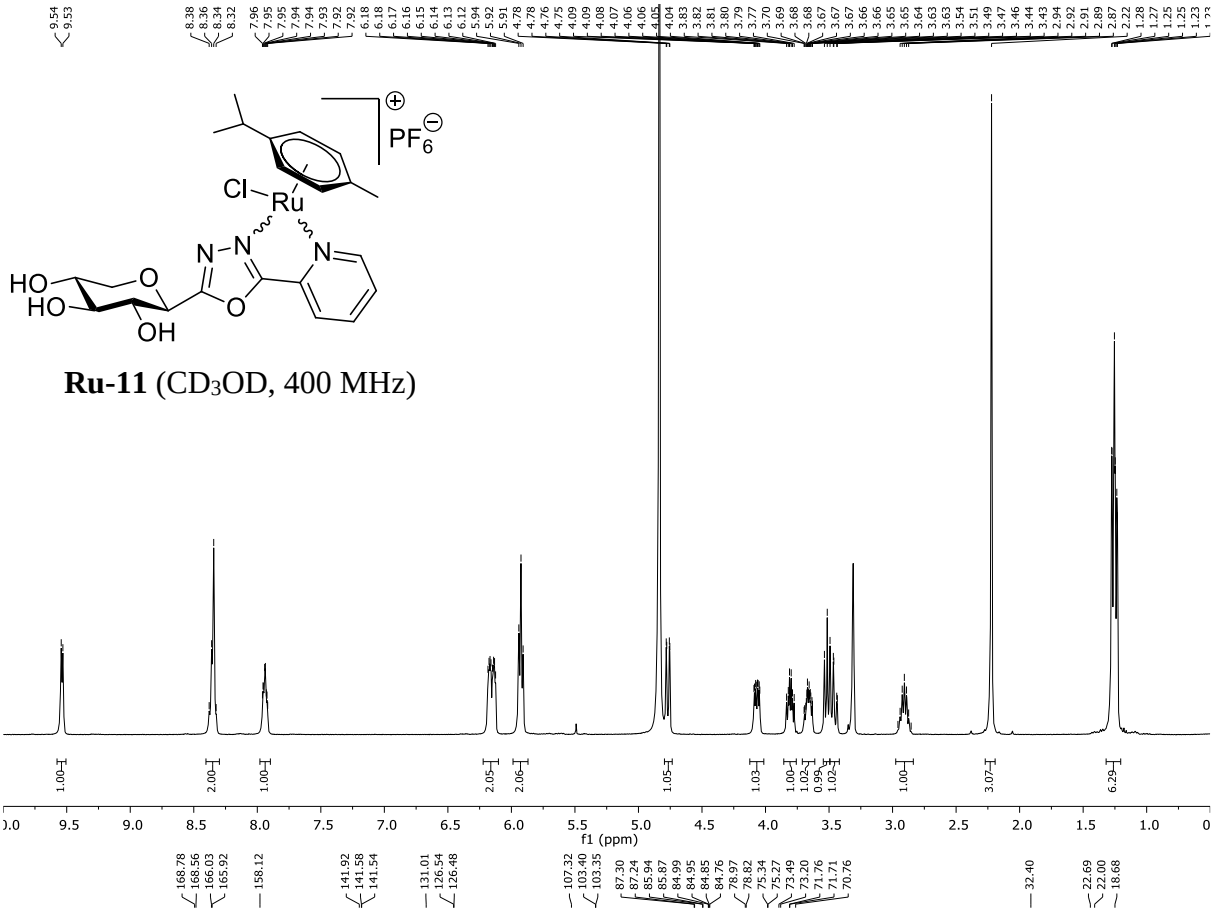

Ru-11 (CD_3OD, 400 MHz)

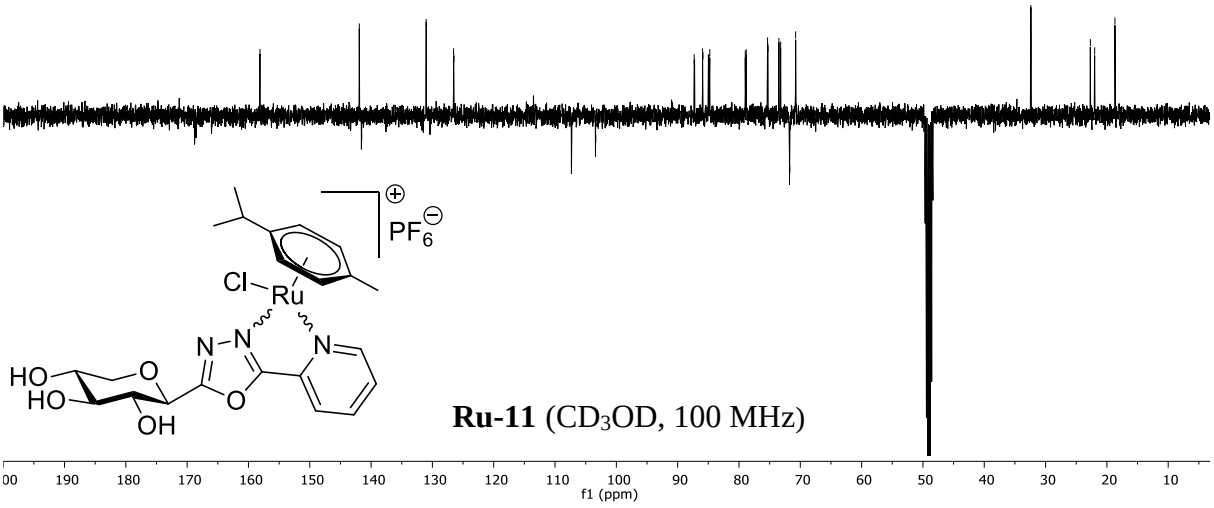

Ru-11 (CD_3OD, 100 MHz)

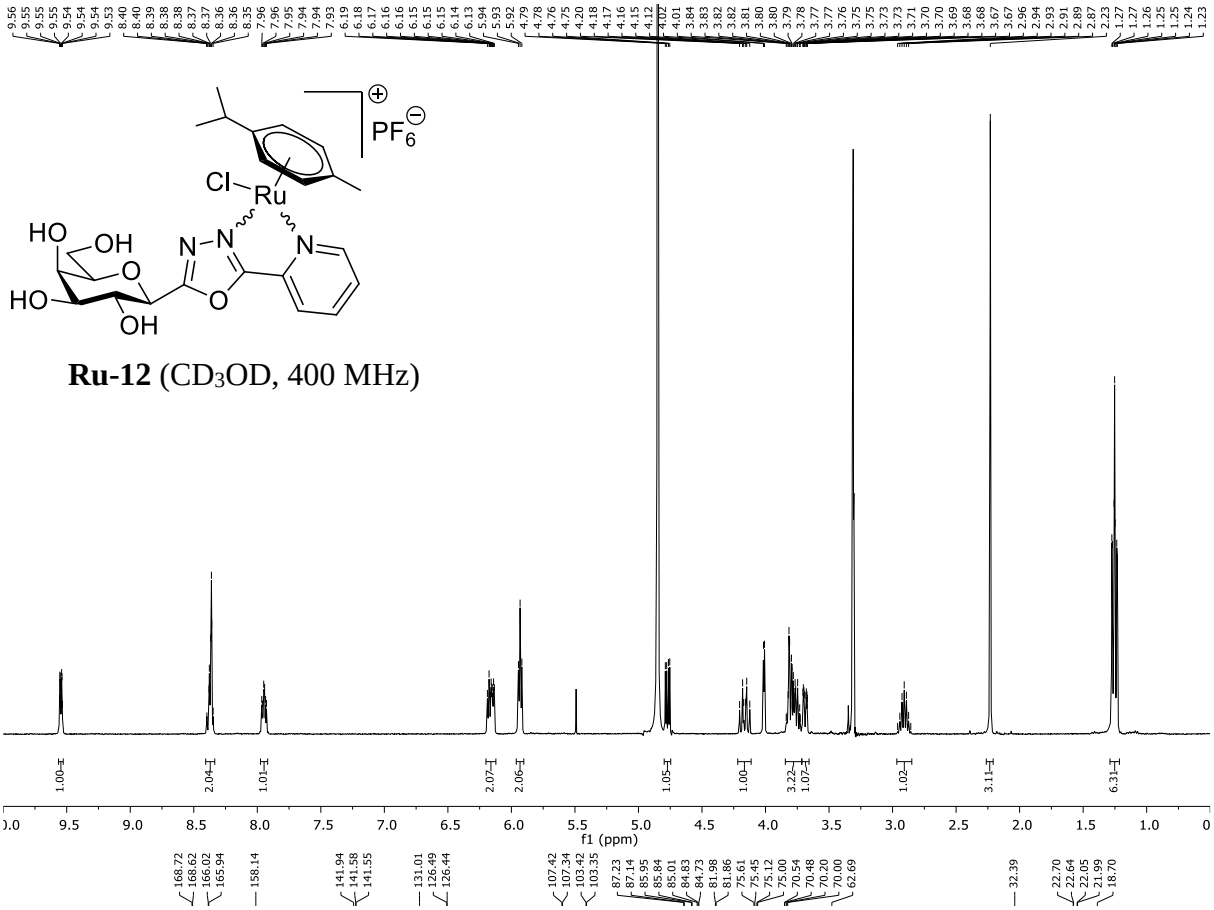

Ru-12 (CD_3OD, 400 MHz)

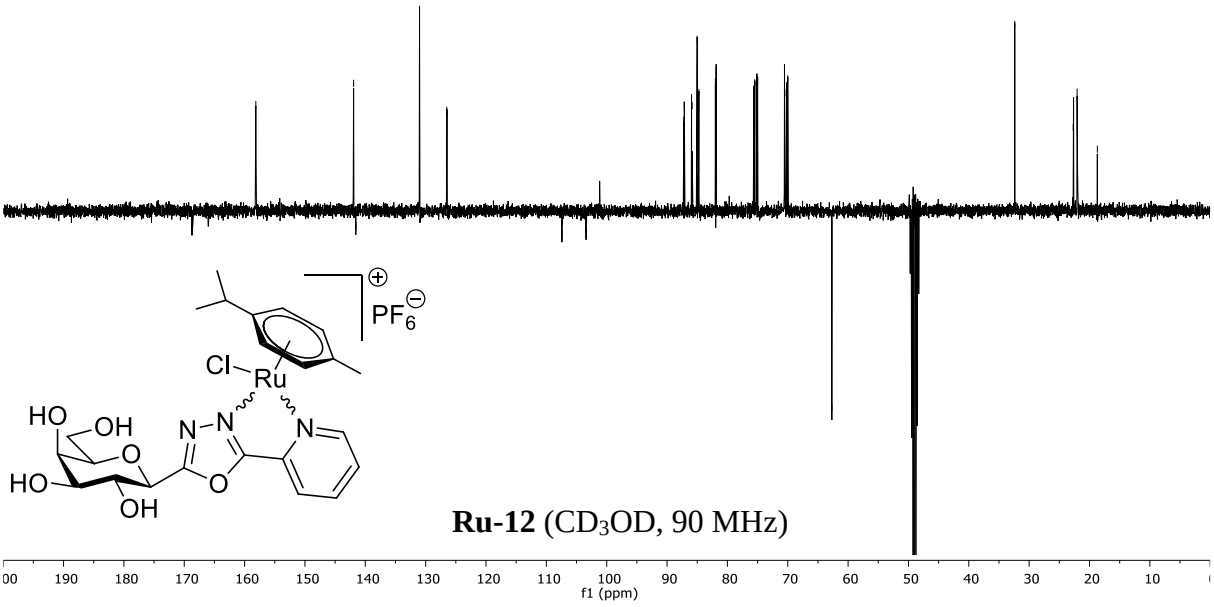

Ru-12 (CD_3OD, 90 MHz)

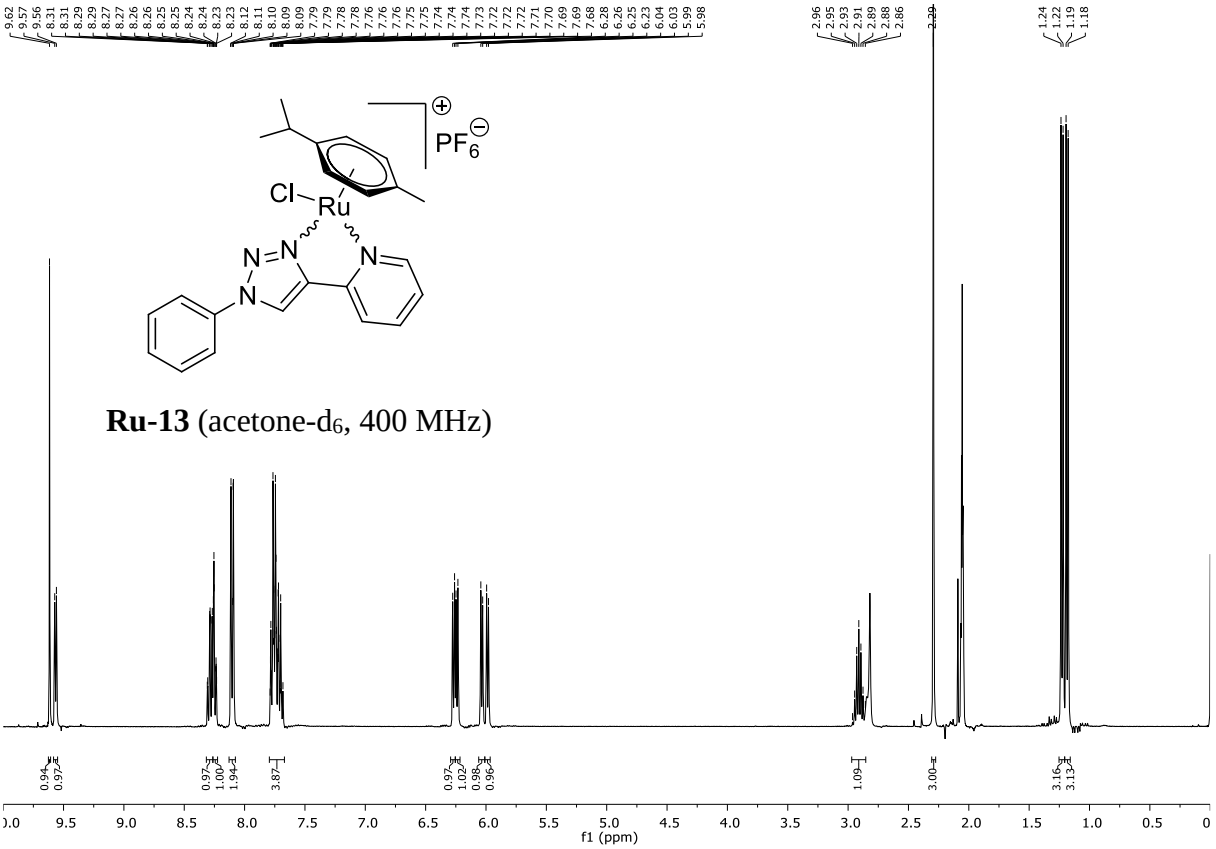

Ru-13 (acetone-d_6, 400 MHz)

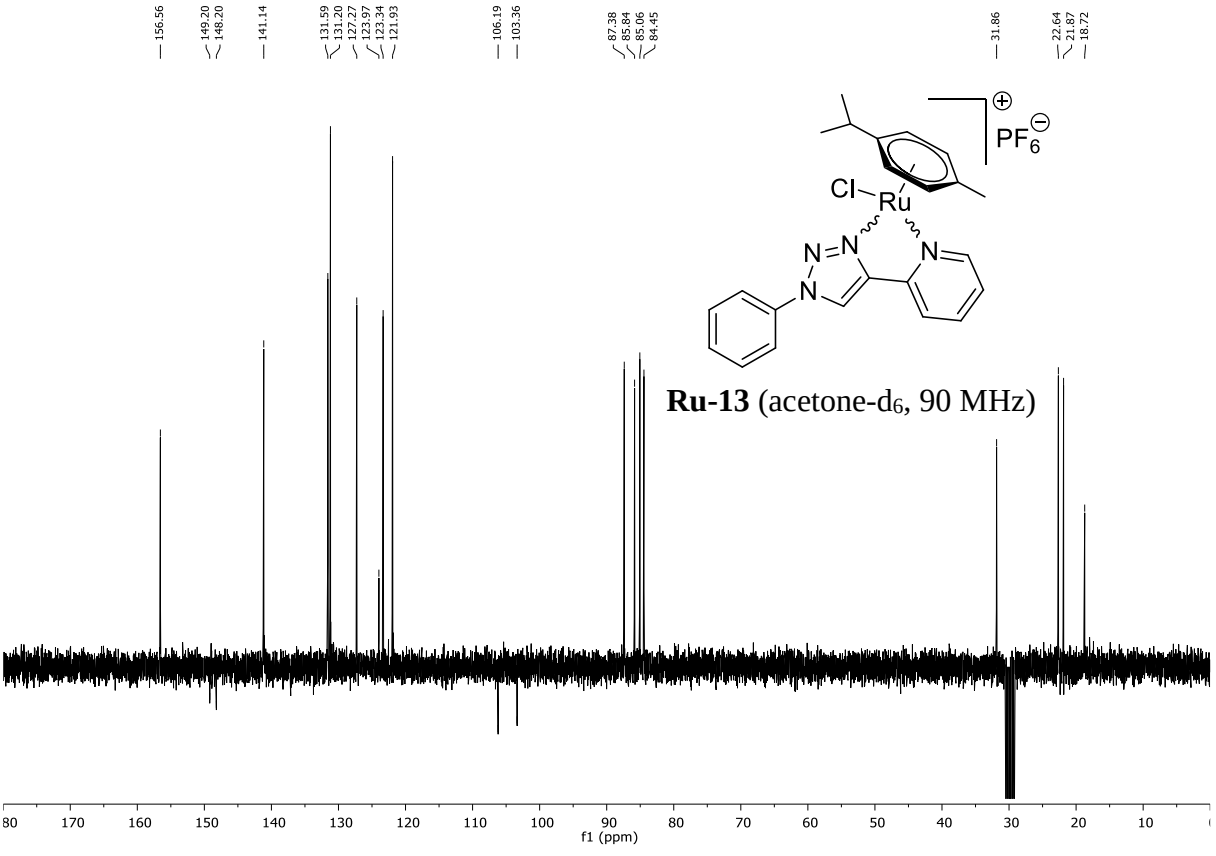

Ru-13 (acetone-d_6, 90 MHz)

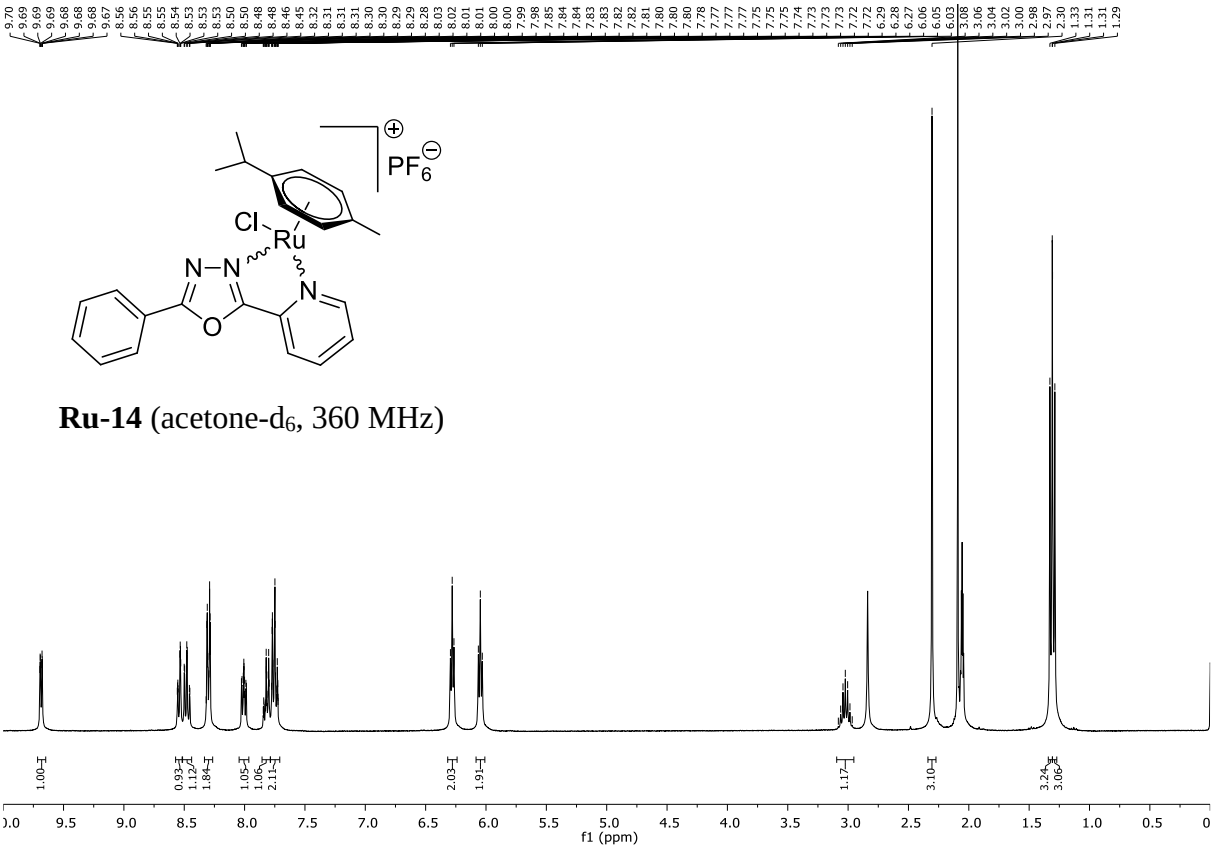

Ru-14 (acetone-d_6, 360 MHz)

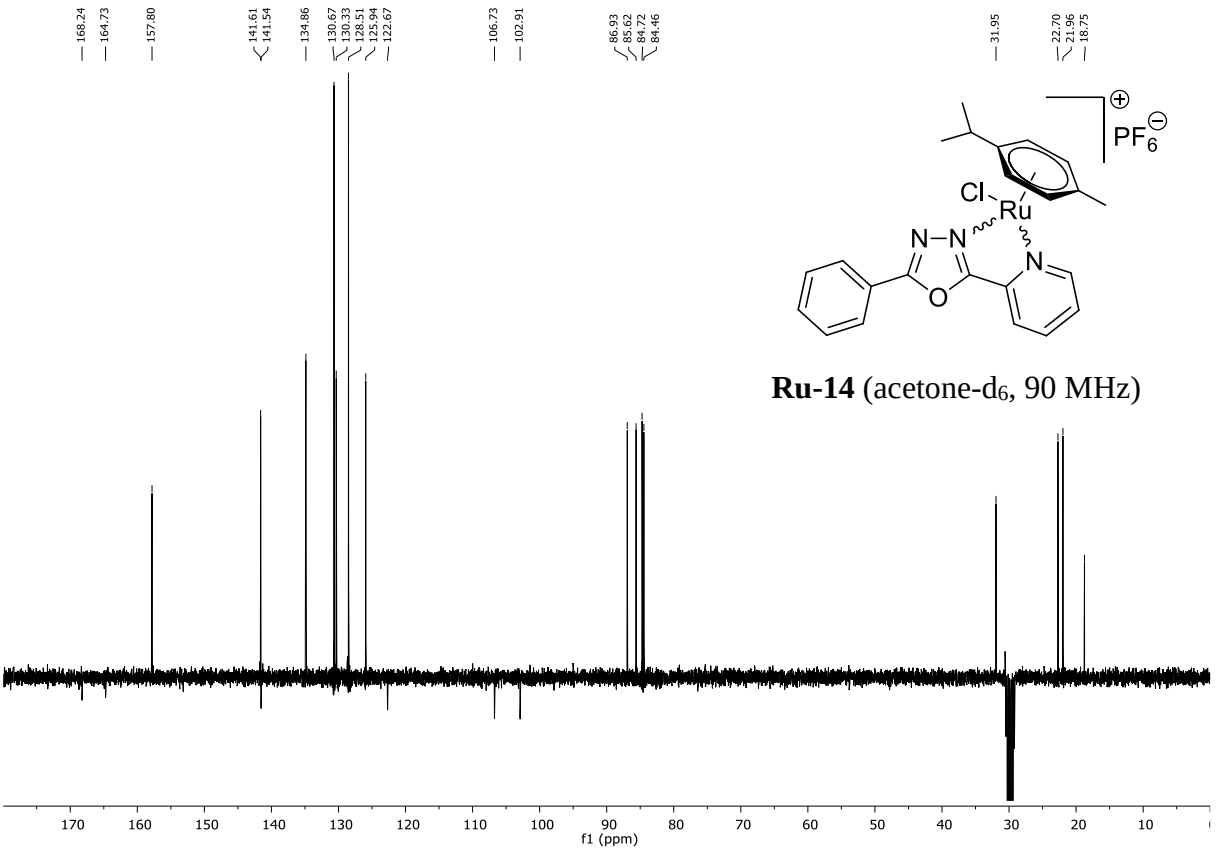

Ru-14 (acetone-d_6, 90 MHz)

3. A representative example for the stability of the complexes in aqueous medium

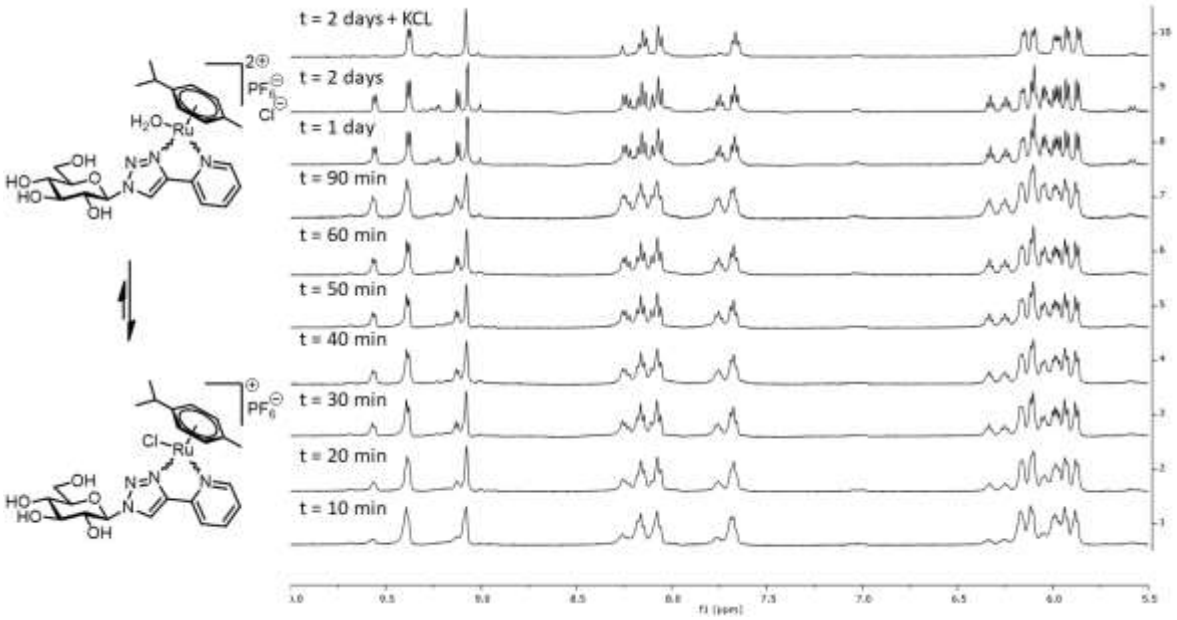

Figure S1. Time dependence of the ^{1}H NMR spectra of **Ru-3a** in D_2O over a 2 day period. By the addition of KCl (100 eq.) the original spectrum could be recovered indicating only Cl^{-}/D_2O exchange during the period of time of the study.

4. Table S9. Distribution coefficient of the synthesized complexes (logD)

Complex		LogD	Complex		logD
Ru-1a	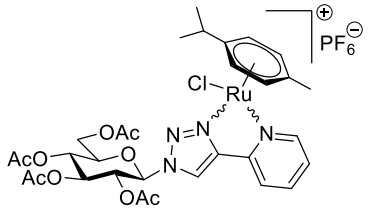	-1.09	**Ru-7**	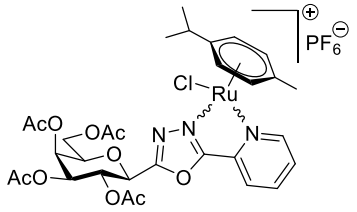	-1.29
Ru-1b	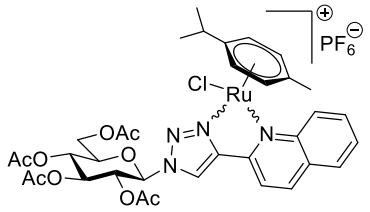	-0.97	**Ru-8**	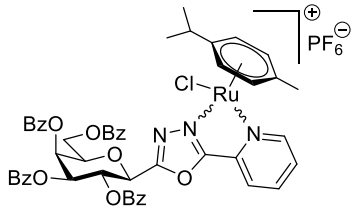	2.44
Ru-2a	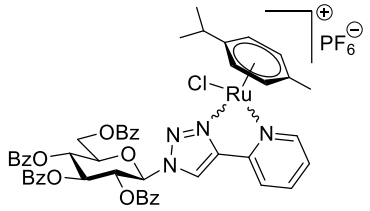	2.85	**Ru-9**	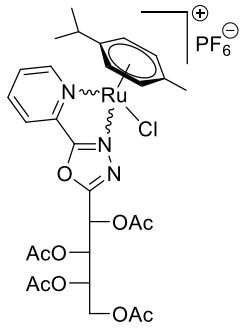	-1.35
Ru-3a	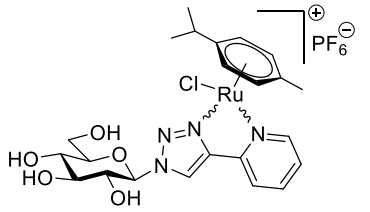	-1.85	**Ru-10**	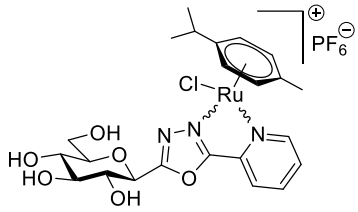	-1.93
Ru-3b	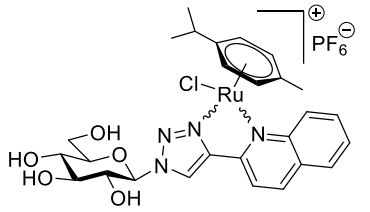	-1.30	**Ru-11**	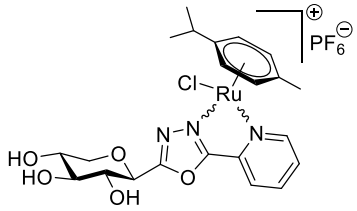	-1.73
Ru-4	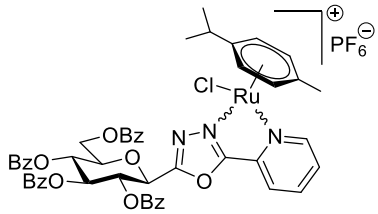	2.41	**Ru-12**	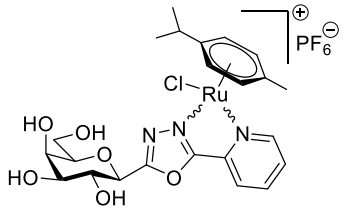	-1.73
Ru-5	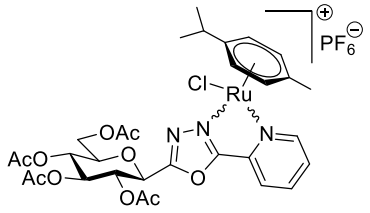	-1.80	**Ru-13**	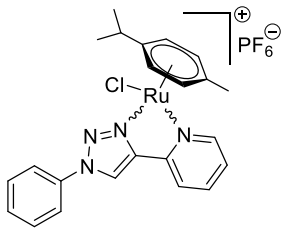	0.44
Ru-6	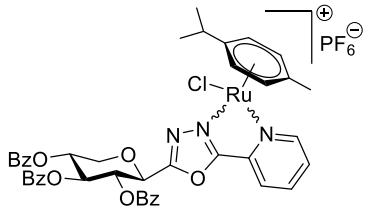	2.04	**Ru-14**	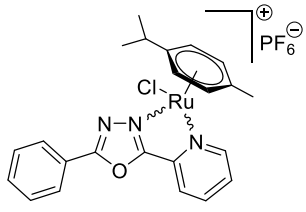	1.63